

A Roadmap to Interstellar Flight

Philip Lubin

Physics Dept, UC Santa Barbara

lubin@deepspace.ucsb.edu

submitted to JBIS April 2015

Abstract – In the nearly 60 years of spaceflight we have accomplished wonderful feats of exploration and shown the incredible spirit of the human drive to explore and understand our universe. Yet in those 60 years we have barely left our solar system with the Voyager 1 spacecraft launched in 1977 finally leaving the solar system after 37 years of flight at a speed of 17 km/s or less than 0.006% the speed of light. As remarkable as this we will never reach even the nearest stars with our current propulsion technology in even 10 millennium. We have to radically rethink our strategy or give up our dreams of reaching the stars, or wait for technology that does not exist. While we all dream of human spaceflight to the stars in a way romanticized in books and movies, it is not within our power to do so, nor it is clear that this is the path we should choose. We posit a technological path forward, that while not simple, it is within our technological reach. We propose a roadmap to a program that will lead to sending relativistic probes to the nearest stars and will open up a vast array of possibilities of flight both within our solar system and far beyond. Spacecraft from gram level complete spacecraft on a wafer (“wafersats”) that reach more than $\frac{1}{4} c$ and reach the nearest star in 15 years to spacecraft with masses more than 10^5 kg (100 tons) that can reach speeds of greater than 1000 km/s. These systems can be propelled to speeds currently unimaginable with existing propulsion technologies. To do so requires a fundamental change in our thinking of both propulsion and in many cases what a spacecraft is. In addition to larger spacecraft, some capable of transporting humans, we consider functional spacecraft on a wafer, including integrated optical communications, optical systems and sensors combined with directed energy propulsion. Since “at home” the costs can be amortized over a very large number of missions. In addition the same photon driver can be used for planetary defense, beamed energy for distant spacecraft as well as sending power back to Earth as needed, stand-off composition analysis, long range laser communications, SETI searches and even terra forming. The human factor of exploring the nearest stars and exo-planets would be a profound voyage for humanity, one whose non-scientific implications would be enormous. It is time to begin this inevitable journey beyond our home.

Introduction: Nearly 50 years ago we set foot on the surface of the moon and in doing so opened up the vision and imaginations of literally billion of people. The number of children ennobled to dream of spaceflight is truly without equal in our history. Many reading this will remember this event or look back at the grainy images with optimism for the future. At the same time we sent robotic probes throughout our solar system and took images of distant galaxies and exoplanet signatures that are forever engrained in our minds. One of humanities grand challenges is to explore other planetary systems by remote sensing, sending probes, and eventually life to explore. Within 20 light-years of the Sun, there are over 150 stars including white and brown dwarfs and there are known to be a number of planets around at least 12 of these stars and at least 17 stars in 14 star systems appear to be capable of supporting planets in stable orbits within the "habitable zone". This is an incredibly rich environment to explore. Even within the outer reaches of our solar system and into the beginnings of interstellar space lay a profoundly interesting number of topics we would love to explore if we could. These include the Oort cloud, heliosheath and heliopause, the solar gravitational lens focus (actually a line) among others. While a decade ago what we propose would have been pure fantasy. **It is no longer fantasy.** Recent dramatic and poorly-appreciated technological advancements in directed energy have made what we

propose possible, though difficult. **There has been a game change in directed energy technology whose consequences are profound for many applications including photon driven propulsion. This allows for a completely modular and scalable technology without "dead ends".**

We propose a system that will allow us to take the step to interstellar exploration using directed energy propulsion combined with miniature probes including some where we would put an entire spacecraft on a wafer to achieve relativistic flight and allow us to reach nearby stars in a human lifetime. Combined with recent work on wafer scale photonics, we can now envision combining these technologies to allow for a realistic approach of sending probes far outside our solar system and to nearby stars. As a part of our effort we propose a roadmap to allow for staged development that will **allow us not only to dream but to do.** By leaving the main propulsion system back in Earth orbit (or nearby) and propelling wafer scale highly integrated spacecraft that include cameras, bi-directional optical communications, power and other sensors we can achieve gram scale systems coupled with small laser driven sails to achieve relativistic speeds and traverse the distance to the nearest exoplanets in a human lifetime. **While this is not the same as sending humans it is a step towards this goal and more importantly allows us to develop the relevant technological base and the ability to build a single "photon driver" to send out literally millions of low mass probes in a human lifetime.** The key to the system lays in the ability to build both the photon driver and the ultra-low mass probe. Recent developments now make this possible.

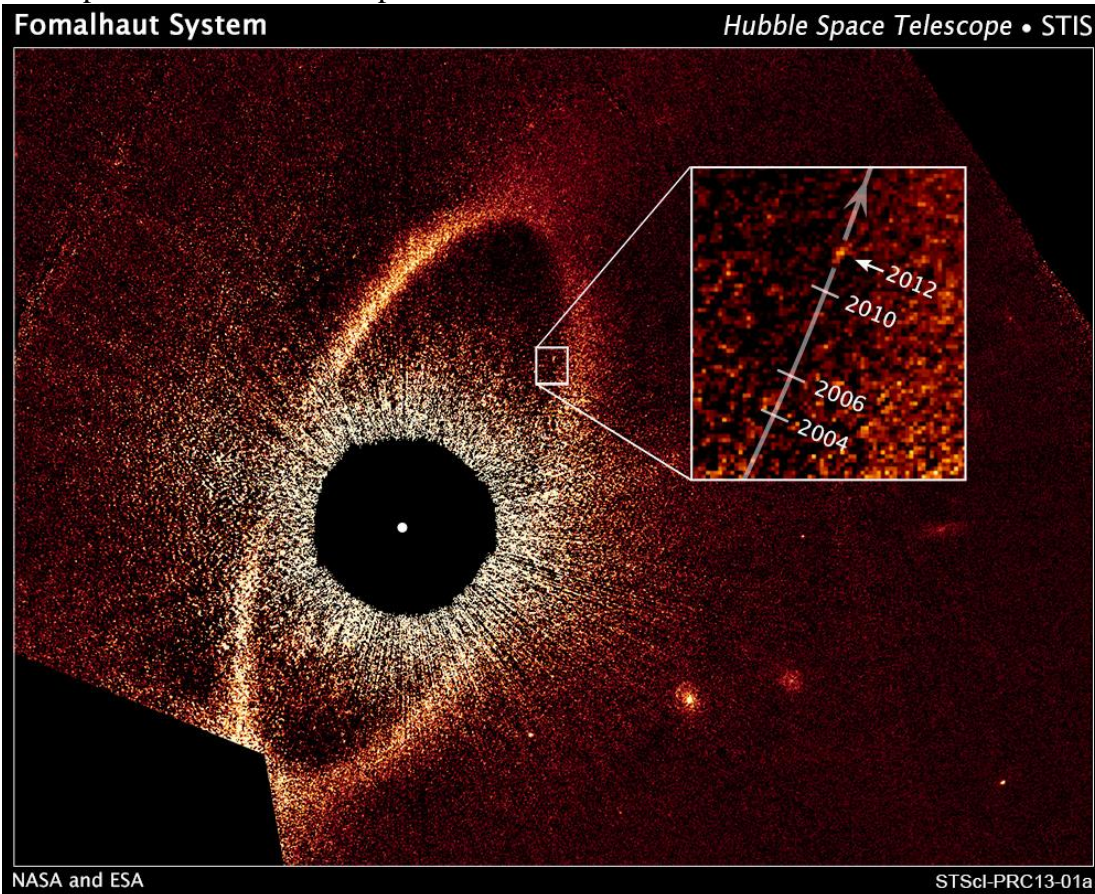


Figure 1 – HST image of the star Fomalhaut indicating a possible exoplanet. This is one possible target that is within reach.

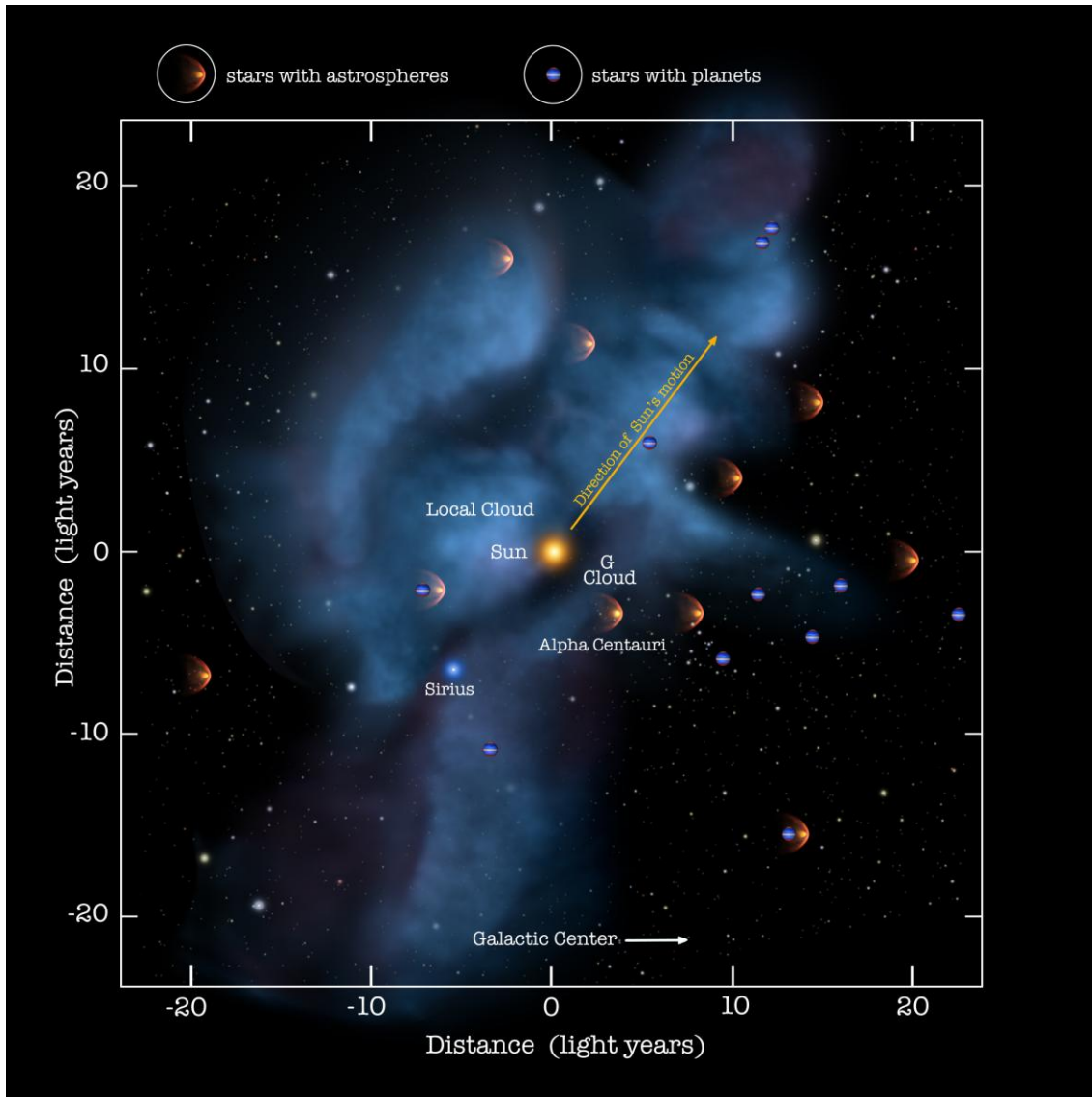


Figure 2 – Stars and structures within about 25 lightyears of the Earth. As indicated some of the stars nearby are already known to contain planets and planetary systems that are potential targets. From Fritsch 2015.

Electromagnetic Acceleration vs Chemical Acceleration: There is a profound difference in what we have been able to do in accelerating material via chemical means vs electromagnetic means. This difference in speeds achieved is dramatically illustrated if we compare the beta (v/c) and gamma factors in this area. We clearly have produce highly relativistic systems but only at the particle level. Practical systems need to be macroscopic as we do not currently have the technological means to self assemble relativistic particle into macroscopic systems. Electromagnetic acceleration is only limited by the speed of light while chemical systems are limited to the energy of chemical processes which are typically of order 1 eV per bond or molecule. To reach relativistic speeds we would need GeV per bond equivalent or about a billion times larger than chemical interactions.

We propose electromagnetic acceleration to achieve relativistic speeds for macroscopic objects but not using conventional accelerators but using light to directly couple to macroscopic objects. This is simply using a very intense light source to accelerate matter. This has the additional advantage of leaving the propulsion source behind to greatly reduce the spacecraft mass. Of course, this has the disadvantage of

reducing or eliminating (depending on the system design) maneuverability once accelerated. For many systems this is not acceptable so hybrid systems are proposed as well as pure photon driven systems. While photon drive is not a new concept (solar sails, laser sails etc) what is new is that directed energy photonic technology has recently progressed to the point where it is now possible to begin the construction of systems to accelerate macroscopic systems to relativistic speeds. Reaching relativistic speeds with macroscopic systems would be a watershed in our path to the stars.

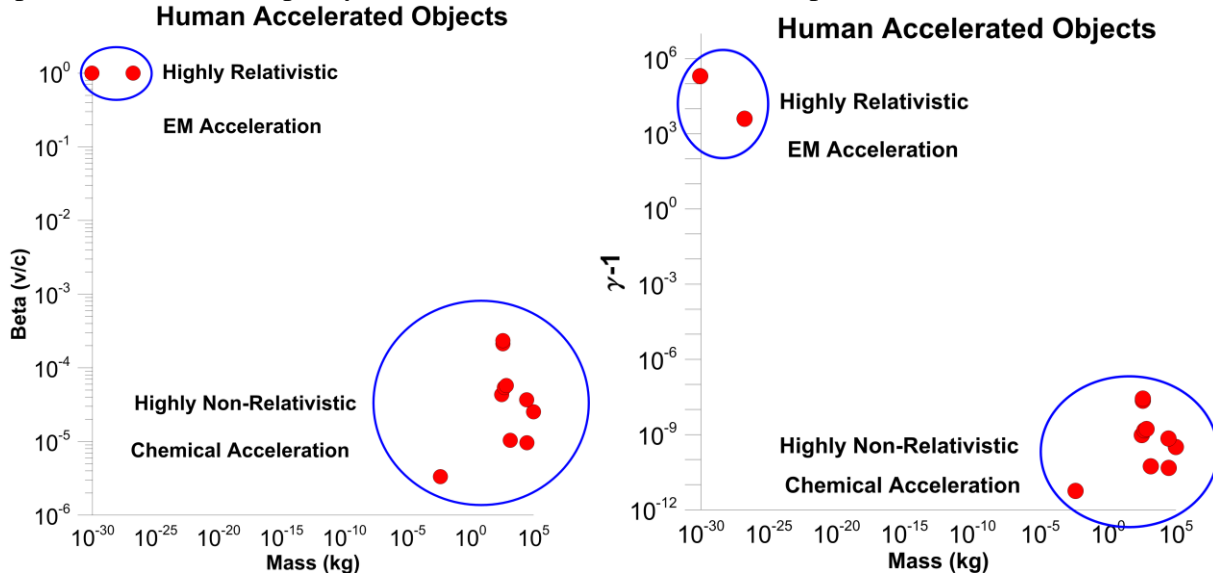


Figure 3 – Left – Fractional speed of light achieved by human accelerated objects vs mass of object from sub atomic to large macroscopic objects. Right – The same but showing $\gamma-1$ where γ is the relativistic “gamma factor”. $\gamma-1$ times the rest mass energy is the kinetic energy of the object.

While a decade ago what we propose would have been pure fantasy. **It is no longer fantasy.** Recent dramatic and poorly-appreciated technological advancements in directed energy have made what we propose possible, though difficult. **There has been a game change in directed energy technology whose consequences are profound for many applications including photon driven propulsion. This allows for a completely modular and scalable technology without "dead ends".**

This will allow us to take the step to interstellar exploration using directed energy propulsion combined with miniature probes including some where we would put an entire spacecraft on a wafer in some cases to achieve relativistic flight and allow us to reach nearby stars in a human lifetime.



Figure 4 – Artistic rendition of a laser driven spacecraft. Pictorial only.

Photon Driver – Laser Phased Array: The key to the system lays in the ability to build the photon driver. For relativistic flight ($>0.1 c$) development of ultra-low mass probes is also needed. Recent developments now make this possible. The photon driver is a laser phased array which eliminates the need to develop one extremely large laser and replaces it with a large number of modest (kW class) laser amplifiers that are inherently phase locked as they are fed by a common seed laser. This approach also eliminates the conventional optics and replaces it with a phased array of small optics that are thin film optical elements. Both of these are a follow on DARPA programs and hence there is enormous leverage in this system. The laser array has been described in a series of papers we have published and is called **DE-STAR (Directed Energy System for Targeting of Asteroids and ExploRation)**. **Powered by the solar PV array the same size as the 2D modular array of modest and currently existing kilowatt class Yb fiber-fed lasers and phased-array optics it would be capable of delivering sufficient power to propel a small scale probe combined with a modest (meter class) laser sail to reach speeds that are relativistic.** DE-STAR units are denoted by numbers referring to the log of the array size in meters (assumed square). Thus DE-STAR-1 is 10 m on a side, -2 is 100 m, *etc.* Photon recycling (multiple bounces) to increase the thrust is conceivable but it NOT assumed. The modular sub systems (baselined here at 1-4 m in diameter) fit into current launchers such as the upcoming SLS and while deployment of the full system is not our goal in the short term, smaller version could be launched to test proof of concept. **As an example, on the eventual upper end, a full scale DE-STAR 4 (50-70 GW) will propel a wafer scale spacecraft with a 1 m laser sail to about 26% the speed of light in about 10 minutes (20 kg_o accel), reach Mars (1 AU) in 30 minutes, pass Voyager I in less than 3 days, pass 1,000 AU in 12 days and reach Alpha Centauri in about 15 years.** The same directed energy driver (DE-STAR 4) can also **propel a 100 kg payload to about 2% c and a 10,000 kg payload to more than 1,000 km/s.** While such missions would be truly amazing, the system is scalable to any level of power and array size where the tradeoff is between the desired mass and speed of the spacecraft. Our roadmap will start with MUCH more modest systems including ground based tests, CubeSat tests, possibly ISS tests and increasingly sophisticated systems. Useful testing can begin at the sub kilowatt level as the system is basically "self-similar" with all arrangements being essentially scaled versions of the others. There is no intrinsic barrier to the speed, except the speed of light, and thus unlike other technologies there is no

"dead end". On the lower end kilowatt or even 100 W class tests can be conducted to propel very small sub mm payloads to 10 km/s and to meter scale to ~100 m/s. **This technology is scalable over an enormous range of mass scales.** The "laser photon driver" can propel virtually any mass system with the final speed only dependent on the scale of the driver built. Accelerating small 10 μ m "grains" to Mach 1000 for hypersonic tests would interest a lot of people, for example. **Once built the system can be amortized over a very large range of missions allowing literally hundreds of relativistic wafer scale payload launches per day (~40,000/yr or one per sq deg on the sky) or 100-10,000 kg payloads for interplanetary missions at much slower rates (few days to weeks).** For reference 40,000 wafers/ and reflectors, enough to send one per square degree on the entire sky, have a total mass of only 80kg. No other current technology nor any realistically envisioned opens this level of possibility. While worm holes, antimatter drives and warp drives may someday be reality they are not currently, nor do we have a technological path forward to them. Directed energy propulsion allows a path forward to true interstellar probes. The laser array technology is modular and extensible allowing a logical and well defined roadmap with immediate probe tests to start exploring the interstellar medium on the way to the nearest stars. **This technology is NOT science fiction. Things have changed.** The deployment is complex and much remains to be done but it is time to begin. Since the system is modular and scalable the costs to begin are very modest as even small systems are useful. The same system can be used for many other applications as outlined in our papers which amortizes the costs over multiple tasks.

Exploring the Interstellar Medium (ISM) - On the development path to the nearest stars lay a wealth of information at the edge of and just outside our solar system. It is not "all or nothing" in going outside of our solar system. We will have many targets, including the solar system plasma and magnetic fields and its interface with the ISM, the heliopause and heliosheath, the Oort cloud outside and Kuiper belt inside, asteroids, KBO's, solar lens focus where the Sun acts as a gravitational lens to magnify distant objects. A more modest mission at 200 km/s (40 AU/yr) would be wonderful for ISM studies.

Power levels and efficiency - Our systems can be designed and tested at any power level but it is worth comparing the power levels with conventional flight systems such as the previous Shuttle system. Each Shuttle solid rocket booster (SRB) is 12.5 MN thrust with an exhaust speed of 2.64 km/s and burns for 124 seconds with an ISP of 269 s. The main engine (H₂/O₂) has 5.25 MN thrust with an exhaust speed of 4.46 km/s and burns for 480 s with an ISP of 455 s. The "power" of each SRB is thus about 17 GW. This language is not commonly used but is instructive here. The main engine has a power of about 11 GW and thus at liftoff the Shuttle consumed about 45 GW of chemical power or very similar to the largest systems we have studied (DE-STAR 4) and that required for interstellar missions. The total energy expended to get the orbiter plus the maximum payload to LEO is about 9.4×10^{12} J = 9.4 TJ. The kinetic energy (KE) of the orbiter + payload at LEO is about 4.0 TJ. The efficiency (KE at LEO/ total launch energy) is about 43%. Compare this to a 1 g wafer and a 1 g reflector travelling at 26% c for one of our many missions. This KE is about 3.0 TJ and the integrated efficiency is about 26% or nearly identical to the Shuttle at LEO. It is not surprising that the amount of power needed for the laser drive is similar to that required by the Shuttle. Shuttle propulsion technology cannot get us to the stars but directed energy can.

Physics of Directed Energy Propulsion. We assume a square diffraction limited phased array of size "d" illuminating a square payload "laser" sail of size "D". The non-relativistic solution for acceleration, speed and distance to where the laser spot equals the payload sail is (Bible 2013, Lubin 2015):

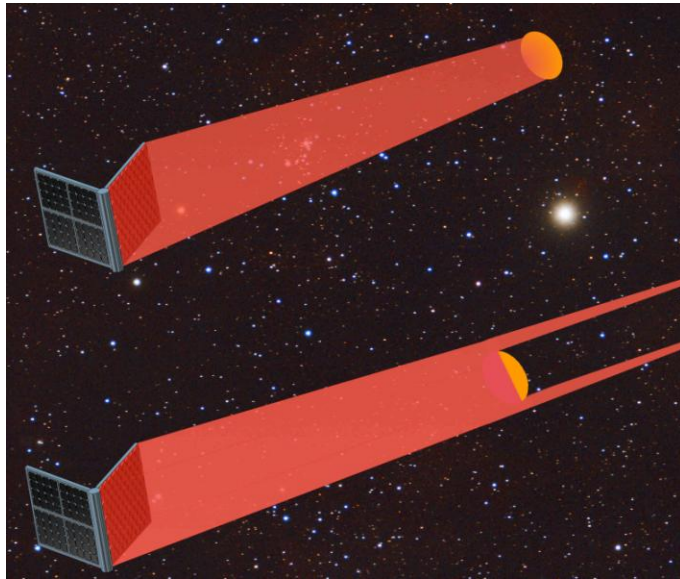


Figure 5 - Conceptual drawing showing beam filling sail and then as distance increases eventually overflowing. With continued illumination speed increases by $2^{1/2}$.

Physics of Photon Driven Propulsion - We solve for the non-relativistic case here and the relativistic case below. We assume a laser power P_0 and a total mass (spacecraft + sail) of m . The detailed solution is given in the appendix. It is summarized here.

$$F = \frac{P_0(1 + \epsilon_r)}{c} = \text{laser thrust on payload with laser power } P_0 \text{ with sail reflection } \epsilon_r$$

while laser spot is smaller than sail

where $\epsilon_r = 0$ for no reflection (all absorbed) and 1 for complete reflection. For our cases $\epsilon_r \sim 1$.

$$a = F / m = \frac{P_0(1 + \epsilon_r)}{mc} = \text{acceleration}$$

$m = m_{\text{sail}} + m_0$ = total mass of sail + base payload mass m_0

$m_{\text{sail}} = D^2 h \rho$ where D =sail size, h = sail thickness, ρ =sail density

$$v_0 = \left(\frac{P_0(1 + \epsilon_r)dD}{c\lambda(D^2 h \rho + m_0)} \right)^{1/2} = \text{speed at point where laser spot = sail size}$$

$$L_0 = \frac{dD}{2\lambda} = \text{distance at which laser spot = sail size}$$

with continued illumination the speed increases by $\sqrt{2}$

$$v_\infty = \left(\frac{2P_0(1 + \epsilon_r)dD}{c\lambda(D^2 h \rho + m_0)} \right)^{1/2}$$

We can show that the maximum speed occurs when the sail mass = payload mass

$$v_{\text{max-}\infty} = \left(\frac{P_0(1 + \epsilon_r)dD}{c\lambda m_0} \right)^{1/2} = \left(\frac{P_0(1 + \epsilon_r)d}{c\lambda D h \rho} \right)^{1/2} = c \left(\frac{P_0(1 + \epsilon_r)}{P_1} \right)^{1/2} \left(\frac{d}{D} \right)^{1/2} = \left(\frac{P_0(1 + \epsilon_r)d}{c\lambda} \right)^{1/2} (h\rho m_0)^{-1/4}$$

where $P_1 \equiv c^3 \lambda h \rho \approx 2.7 \times 10^{16} \text{ watts} \times \lambda(\text{microns}) h(\text{microns}) \rho(\text{g/cc})$

The time to where the laser spot equals the sail size is:

$$t_0 = \frac{v_{0\text{max}}}{a} = \left(\frac{cdD(D^2 h \rho + m_0)}{P_0(1 + \epsilon_r)\lambda} \right)^{1/2}$$

The time to where the laser spot equals the sail size for case where sail mass = payload mass is:

$$t_0 = \left(\frac{2cdD^3 h \rho}{P_0(1 + \epsilon_r)\lambda} \right)^{1/2} = \left(\frac{2cd}{P_0(1 + \epsilon_r)\lambda} \right)^{1/2} \left(\frac{m_0^3}{h\rho} \right)^{1/4}$$

While counter intuitive in the context of solar sails, the highest speed is achieved with the smallest sail and thus smallest payload mass. The laser has very narrow bandwidth so we design the reflector with multi layer dielectric coatings to have ϵ_r very close to one.

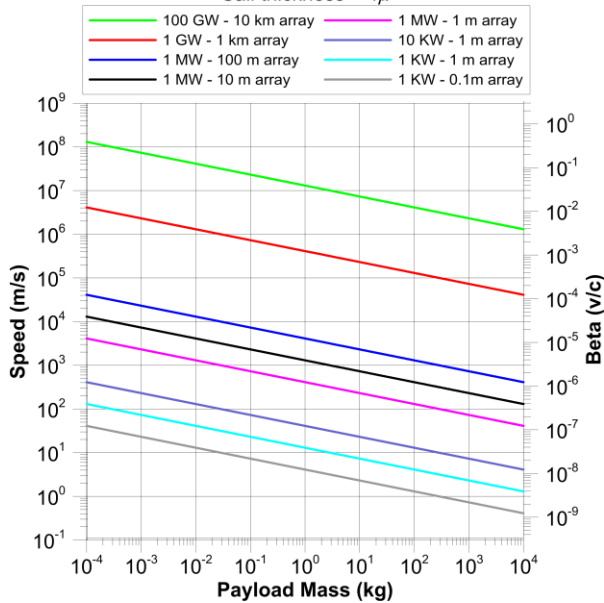
Efficiency - The instantaneous energy efficiency (power that goes into direct kinetic energy/ laser power on reflector) $\epsilon_p = \beta(1 + \epsilon_r) = P_{ot}(1 + \epsilon_r)/mc^2 \sim 2\beta \sim 4P_{ot}/mc^2$ for $\epsilon_r \sim 1$ and total integrated energy efficiency $\epsilon_{\text{total}} = 1/2 \epsilon_p = \beta(1 + \epsilon_r)/2 = P_{ot}(1 + \epsilon_r)^2/2 mc^2 \sim \beta \sim P_{ot}/mc^2$ for $\epsilon_r \sim 1$ where $m = m_{\text{sail}} + m_0$, momentum "eff" = $(1 + \epsilon_r) \sim 2$ for $\epsilon_r \sim 1$ with $\beta \ll 1$. The energy transfer efficiency starts out at very low

levels and then increases proportional to the speed. The total integrated energy efficiency is just 1/2 that of the instantaneous efficiency at the final speed since the force is constant as long as the laser spot is smaller than or equal to the reflector size and hence the acceleration is constant and hence speed increases proportional to time ($\beta \sim t$) and hence the average β is 1/2 the maximum β achieved. This is for the non relativistic case. For spacecraft accelerated to high speeds the energy efficiency can become quite high.

Photon recycling for larger thrust and efficiency - The efficiency of the photon drive can be improved by reusing the photons reflected by the spacecraft reflector in an effective optical cavity mode to get multiple photon reflections. This is known as photon recycling. It is not a new concept but may be of some use for some of our applications. We will see it greatly complicates the system optics however. In the case of photon recycling the photons bounce back and forth in an optical cavity one end of which is the spacecraft reflector and the other end is a relatively more massive (referred to here as fixed) mirror. The total power at the spacecraft mirror sets the force on the spacecraft. The total power on spacecraft mirror is essentially the same as that on the fixed mirror. The combination of the two mirrors forms an optical cavity whose Q factor is defined as $Q = 2\pi E_{\text{cav}}/E_{\text{loss}} \sim \nu/\delta\nu$ where E_{cav} = Energy stored in cavity and E_{loss} = energy lost per cycle and ν is the optical frequency and $\delta\nu$ is the FWHM bandwidth of the resonance . One cycle is the round trip travel time of the light or $2L/c$ where L is the distance between the spacecraft and fixed mirror. In general the fixed mirror will be at the laser driver (ie near the earth). The energy lost per cycle is due to a variety of effects such as increase of kinetic energy of the spacecraft and fixed mirror per cycle, energy lost to mirror(s) absorption per cycle due to non unity reflection coefficient, diffraction effects as the spacecraft moves away and mirror misalignments. For the spacecraft close to the laser optical cavities are possible and do improve efficiency (the effective power on the spacecraft reflector increases by the number of "bounces". As the spacecraft begins to move far away diffraction becomes extremely problematic as do mirror alignment issues and hence photon recycling has much less practical use. It is an area we are exploring but it greatly increases the complexity of the system.

Speed vs Payload Mass and System Parameters

Optimized for Payload Mass = Sail Mass
Sail thickness = 1μ



Speed vs Laser Power and Spacecraft Sail Size

Optics Size = 1 m - Sail thickness = 1μ
Spacecraft mass=0

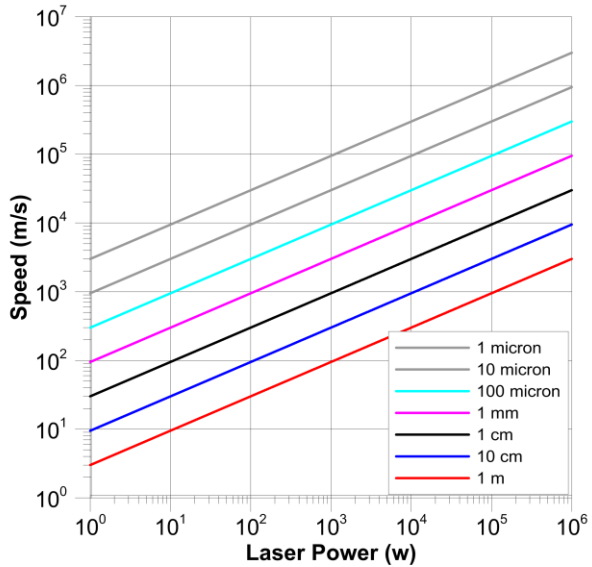
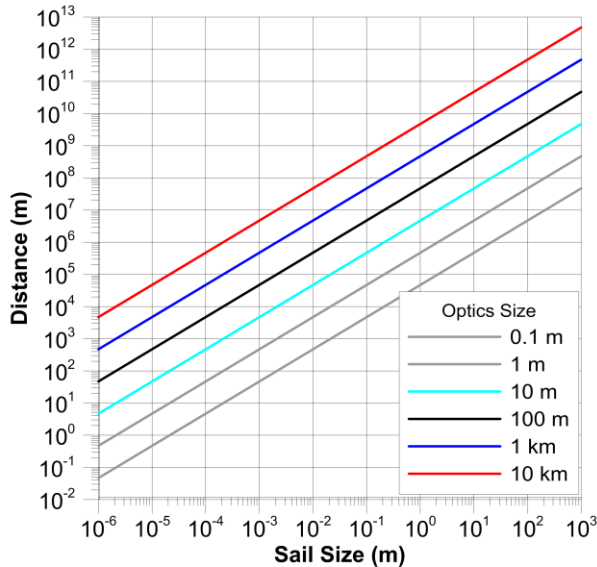


Figure 6 - Left: Speed and Beta vs payload mass vs laser array power and size for systems from very small to very large. This range of systems represents a portion of the roadmap. Right: Speed vs laser power for small systems with 1 m optical aperture vs. sail size. A similar plot exists for a CubeSat like demo mission.

Distance vs Optics Size vs Spacecraft Sail Size Illumination Time vs Laser Power and Reflector Size

Sail thickness = 1μ



Optics Size = 1 m - Reflector thickness = 1μ
Reflector mass only

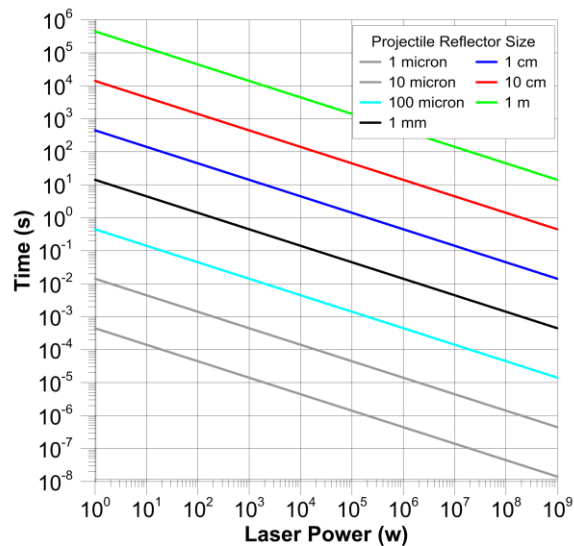


Figure 7 - Left - Distance within which the laser spot size is within the reflector size vs reflector size as well as system optical array size. Right - Acceleration time while the laser spot is within the reflector size vs power and reflector size.

Relativistic solution - We derive the relativistic solution in our papers (Bible et al 2013, Lubin 2015). It is given by t vs β (v/c) and $\gamma=(1-\beta^2)^{-1/2}$ as follows:

$$t = \frac{m_0 c^2}{2P_0(1+\epsilon_r)} \left[\frac{\beta}{1-\beta^2} + \frac{1}{2} \ln \left| \frac{1+\beta}{1-\beta} \right| \right] = \frac{m_0 c^2}{2P_0(1+\epsilon_r)} \left[\gamma^2 \beta + \tanh^{-1} \beta \right]$$

$$\text{Define } t_E \equiv \frac{m_0 c^2}{P_0} \rightarrow t = \frac{t_E}{2(1+\epsilon_r)} \left[\gamma^2 \beta + \tanh^{-1} \beta \right]$$

A more complete relativistic solution is given in Kulkarni and Lubin (2016).

Relativistic effects - Relativistic effects need to be considered for the systems we are proposing. There are a variety of effects to be considered. The critical effects of time dilation, length contraction, wavelength (photon energy) change, and effective mass increase can be parametrized by β and γ which are defined as:

$$\gamma = (1-\beta^2)^{-1/2} \quad \text{where } \beta = \frac{v}{c}$$

$$\gamma = \frac{1}{\sqrt{1-(v/c)^2}} = (1-\beta^2)^{-1/2} \rightarrow 1 + \frac{1}{2}\beta^2, \beta \ll 1$$

In the non relativistic limit β is extremely small (v/c) and γ is very close to unity. As shown the corrections for γ differing from unity are relatively small until β becomes close to 1 (speed near the speed of light) . In the limit as $v \rightarrow c$ ($\beta \rightarrow 1$) then $\gamma \rightarrow \infty$ and the relativistic effects become extreme. As an example for a speed of 0.3 c we have $\gamma \sim 1.05$ or a 5% correction.

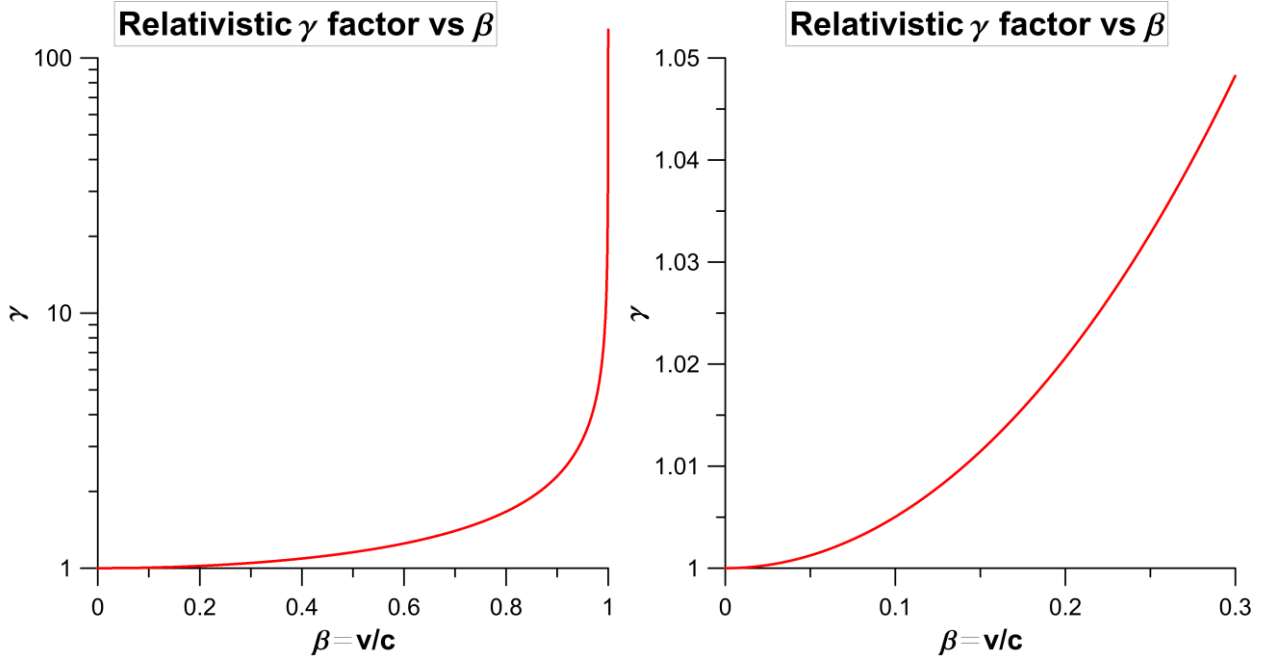


Figure 8 – Relativistic “gamma” factor versus “beta” factor. Gamma goes to infinity as beta goes to unity. Right hand plot restricts range of beta.

Kinetic Energy of Spacecraft - The kinetic energy of the spacecraft increases dramatically with speed. The kinetic energy $KE = m_0 (\gamma-1) c^2$ where the rest mass is m_0 and effective mass $m_{\text{eff}} = m_0 (\gamma-1)$. As the

speed approaches c ($\beta \rightarrow 1$) the kinetic energy diverges to infinity. Hence the problem of propelling non zero rest mass objects at the speed of light. We plot the kinetic energy in both J/kg and megaton TNT (MT) equivalent/ kg vs speed. At $\beta \sim 0.3$ (30% c) the kinetic energy is about 1 MT/kg. Note that modern thermonuclear weapons have an energy release per unit mass of about 5 MT/ton or about 5 kT/kg for large yield weapons. Small yield weapons are much worse than this. **Thus a 1 kg spacecraft going at 0.3 c will have an effective "yield" of 1 MT or roughly that of a large strategic thermonuclear weapon.**

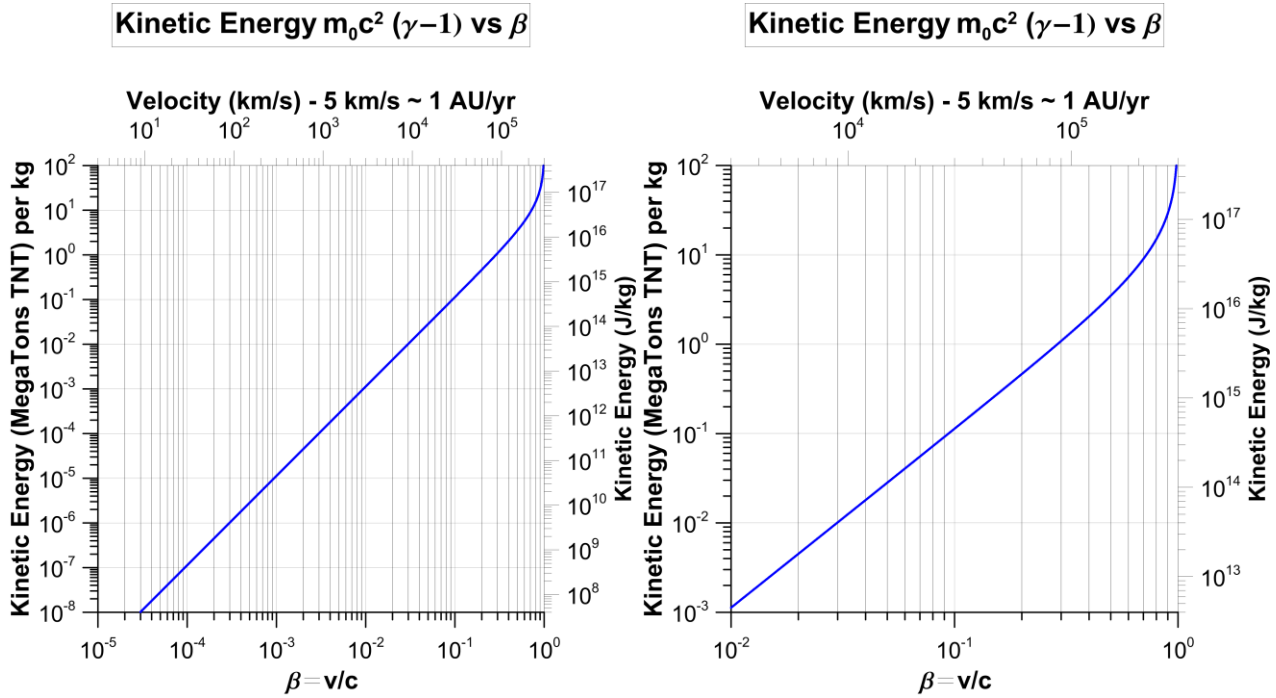


Figure 9 – Kinetic energy vs beta in units of megatons TNT per kg of payload mass as well as Joules per kg. Right hand plot is the same but for a restricted range of beta.

Scaling. Since the system we propose is not single use but rather scalable to any size it is critical to understand the scaling relations in the section above. In general we use the optimized case of payload mass = sail mass and assume a nearly ideal sail tuned to the laser wavelength so $\epsilon_r = 1$. We assume a slightly futuristic sail with thickness of 1 μm for many cases and 10 μm (thick even for today's sails). Future advancements in sails thickness down to 0.1 μm and below can be envisioned but are NOT assumed. They will only make the conclusions even more optimistic. The density of all sails we consider is about the same, namely $\rho \sim 1,400 \text{ kg/m}^3$. We can then vary power, laser array size and payload mass as we proceed along the roadmap from small to large systems. The tradeoffs between payload mass and speed desired and power and array size required are then explored. We cover this much more in our papers but the basic conclusions are as stated - namely payloads from wafer scale and below to 10⁵ kg and above (human capable) can all be propelled, albeit with different speeds. Note the scaling of speed.

$$v_{\text{max-}\infty} = \left(\frac{2P_0 d}{c\lambda} \right)^{1/2} (h\rho m_0)^{-1/4}$$
 which scales as $P_0^{1/2}$, $d^{1/2}$, $h^{-1/4}$, $\rho^{-1/4}$, $m_0^{-1/4}$. The scaling of speed is a mild function of payload mass $\sim m_0^{-1/4}$. This is due to the fact that as the payload mass grows so does

the sail. As the sail grows the acceleration distance increases as the laser spot can become larger. These effects tend to mitigate the increased mass. So while a gram scale wafer can be accelerated to relativistic speeds (26% c in our largest baseline case - DE-STAR 4), the same laser array that allow this also allows propelling a 100 kg craft (Voyager class) to about 1.5% c or nearly 300 times faster than Voyager achieved after 37 years. A 100 kg craft of this time would reach 1AU (~Mars) in about a day while a Shuttle class vehicle with a mass of 10^5 kg (~100 tons) would reach 0.26% c or about 780 km/s or 46 times faster than Voyager. This exceeds the galactic escape speed for example (depending on the Dark Matter distribution). While the numbers may be mind numbing they need to be kept in context. We are NOT proposing we should immediately build the largest system but rather begin the roadmap.

Preliminary System Design: Directed energy systems are ubiquitous, used throughout science and industry to melt or vaporize solid objects, such as for laser welding & cutting, as well as in defense. **Recent advances in photonics now allow for a 2D array of phase locked laser amplifiers fed by a common low power seed laser** that have already achieved near 50% wall plug conversion efficiency and have been built into small phased arrays.

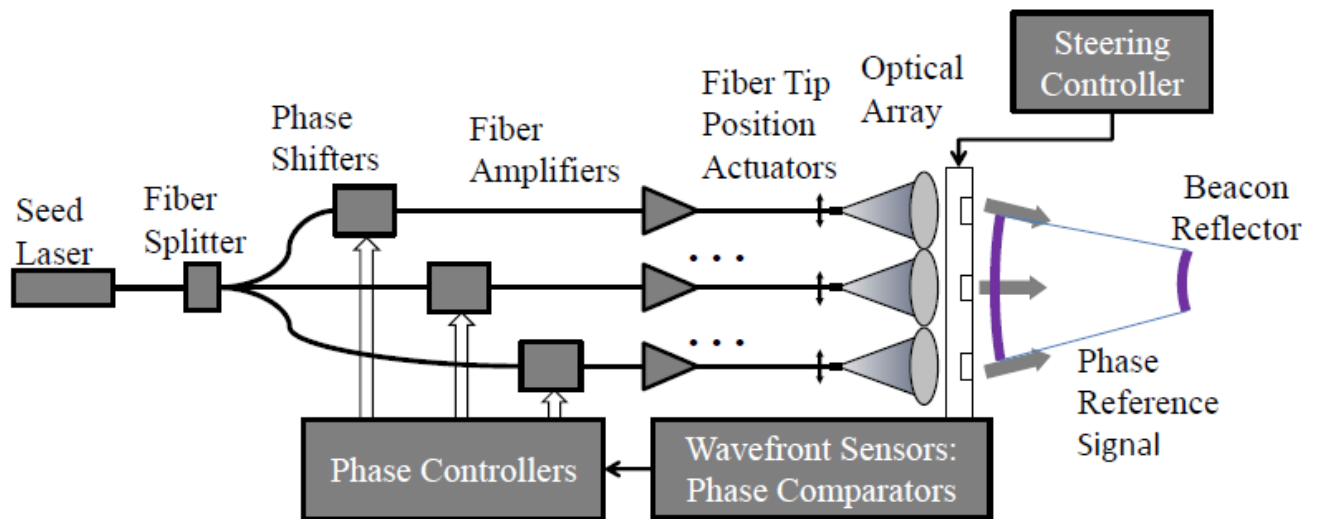


Figure 10 – Schematic design of phased array laser driver. Wavefront sensing from both local and extended systems combined with the system metrology are critical to forming the final beam.

The technology is proceeding on a "Moore's Law" like pace with power per mass at 5 kg/kW with the size of a 1 kW amplifier not much larger than a textbook. There is already a roadmap to reduce this to 1 kg/kW in the next 5-10 years and discussions for advancing key aspects of the technology to higher TRL are beginning. These devices are revolutionizing directed energy applications and have the potential to revolutionize both many related applications. Due to the phased array technology the system can simultaneously send out multiple beams and thus is inherently capable of simultaneous multitasking as well as multi modal. The costs can thus be amortized to greatly reduce the cost per task/ mission.

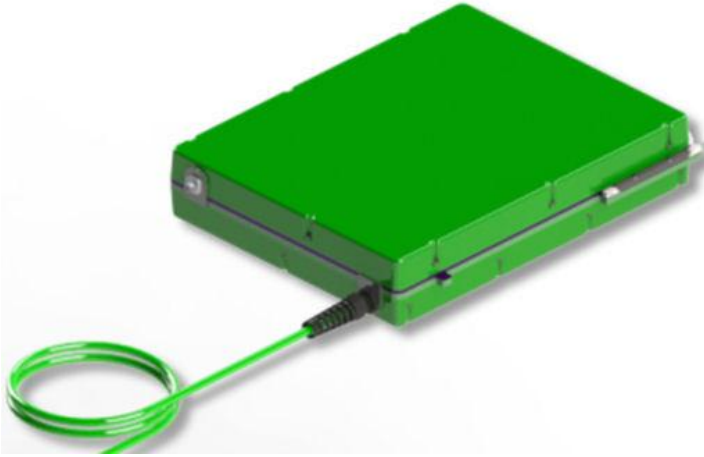


Figure 11 – Picture of current 1-3 kw class Yb laser amplifier which forms the baseline approach for our design. Fiber output is shown at lower left. Mass is approx 5 kg and size is approximately that of this page. This will evolve rapidly but is already sufficient to begin. Courtesy Nufern.

The laser system can be built and tested at any level from desktop to extremely larger platforms. **This is radically different than the older "use a huge laser" approach to photon propulsion.** This is the equivalent to modern parallel processing vs an older single supercomputer.

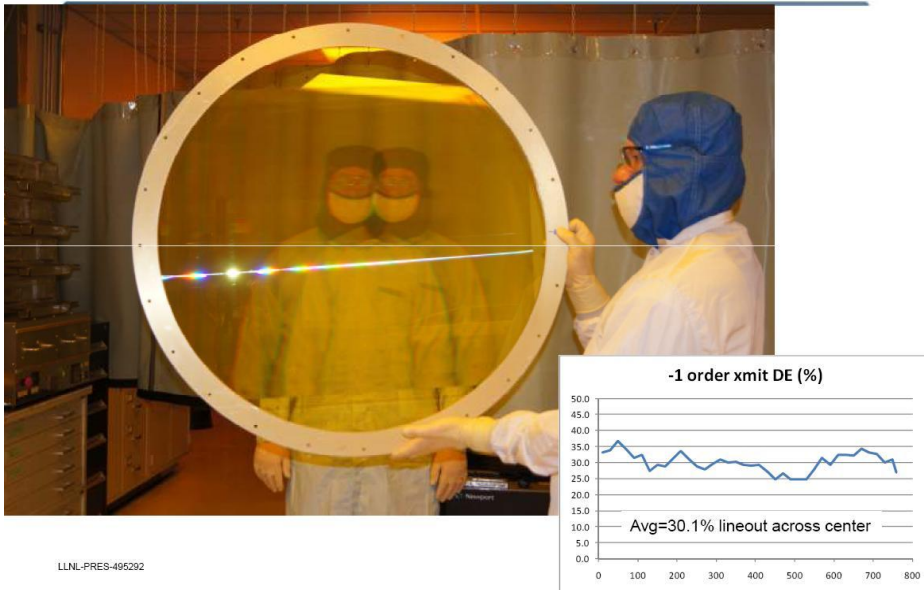


Figure 12 – Thin film replicated optics from DARPA MOIRE Ball-LLNL program. The thin (~ 30 micron) plastic film is replicated from an etched mandrel. Areal mass of the film is approximately 60 g/m² with actual optical mass dominated by mounting ring and not the optic itself. Thin glass and other materials are other optics for these lightweight replicated optics. In our system all optical elements are identical leading to mass production replicated techniques being optimal.

The more modest size systems can be completely tested on the ground as well as sub-orbital flight tested on balloons or possibly sounding rocket. While the largest sized systems (km scale) are required for interstellar missions, small systems have immediate use for roadmap development and applications such as sending small probes into the solar system and then working our way outward as larger laser arrays are built. The laser array is modular, leading to mass production, so that a larger array can be built by

adding elements to a smaller array. **Array testing and propulsion tests are feasible at all levels allowing for roadmap development rather than "all or nothing"**. Small array can also be used for orbital debris removal, ISS defense from space debris as well as stand-on systems for planetary defense so again there is a use at practically every level and funding is well amortized over multiple uses. This allows practical justification for construction. In addition there is an enormous leveraging of DoD and DARPA funds for Directed Energy systems that dramatically lowers the NASA costs.

Phase lockable lasers and current PV performance - New fiber-fed lasers at 1 μm have efficiencies near 40% (DARPA Excalibur program currently at 5 kg/kW with near term goal of 1 kg/kW). We assume incremental efficiency increases to 70% though current efficiencies are already good enough to start the program. It is conceivable that power density could increase to 10 kW/kg in 10-20 years given the current pace. Current space multi-junction PV has an efficiency of nearing 40% with deployable mass per power of less than 7 kg/kW (ATK Megaflex as baselined for DE-STARLITE). Multi junction devices with efficiency in excess of 50% are on the horizon with current laboratory work exploring PV at efficiencies up to 70% over the next decade. We anticipate over a 20 year period PV efficiency will rise significantly, though it is NOT necessary for the roadmap to proceed. The roadmap is relatively "fault tolerant" in technology develop. Array level metrology as a part of the multi level servo feedback system is a critical element and one where recent advances in low cost nanometer level metrology for space applications is another key technology. One surprising area that needs significant work is the simple radiators that radiate excess heat. Currently this is the largest mass sub system at 25 kg/kw (radiated). The increase in laser efficiency reduces the radiator mass as does the possibility to run the lasers well above 300K. Radiation hardening/ resistance and the TRL levels needed for orbital use are another area we are currently exploring.

Wafer Scale Spacecraft. Recent work at UCSB on Si photonics now allows us to design and build a "spacecraft on a wafer". The recent (UCSB) work in phased array lasers on a wafer for ground-based optical communications combined with the ability to combine optical arrays (CMOS imagers for example) and MEMS accelerometers and gyros as well as many other sensors and computational abilities allows for extremely complex and novel systems. Traditional spacecraft are still largely built so that the mass is dominated by the packaging and interconnects rather than the fundamental limits on sensors. Our approach is similar to comparing a laptop of today to a super computer with similar power of 20 years ago and even a laptop is dominated by the human interface (screen and keyboard) rather than the processor and memory. Combining nano photonics, MEMS and electronics with recent UCSB work on Si nano wire thermal converters allows us to design a wafer that also has an embedded RTG or beta converter power source (recent LMCO work on thin film beta converters as an example) that can power the system over the many decades required in space. Combined with small photon thrusters (embedded LEDs/lasers for nN thrust steering on the wafer gives a functional spacecraft. While not suitable for every spacecraft design by any means this approach opens up radically new possibilities. In addition the power from the laser itself can add significant power to the spacecraft even at large distances. We have run link margin calculations including Zodi, CIB, galaxy and optical emission for such a wafer scale system run in a hibernate/ burst mode using the DE-STAR array as both the transmitter of power to propel and communicate with the spacecraft as well as to receive the very weak signal from the spacecraft and conclude it is feasible to receive data (albeit at low rate) at light year distances. For pointing we use the wafer camera to star track and/or lock to DE-STAR laser as a beacon.

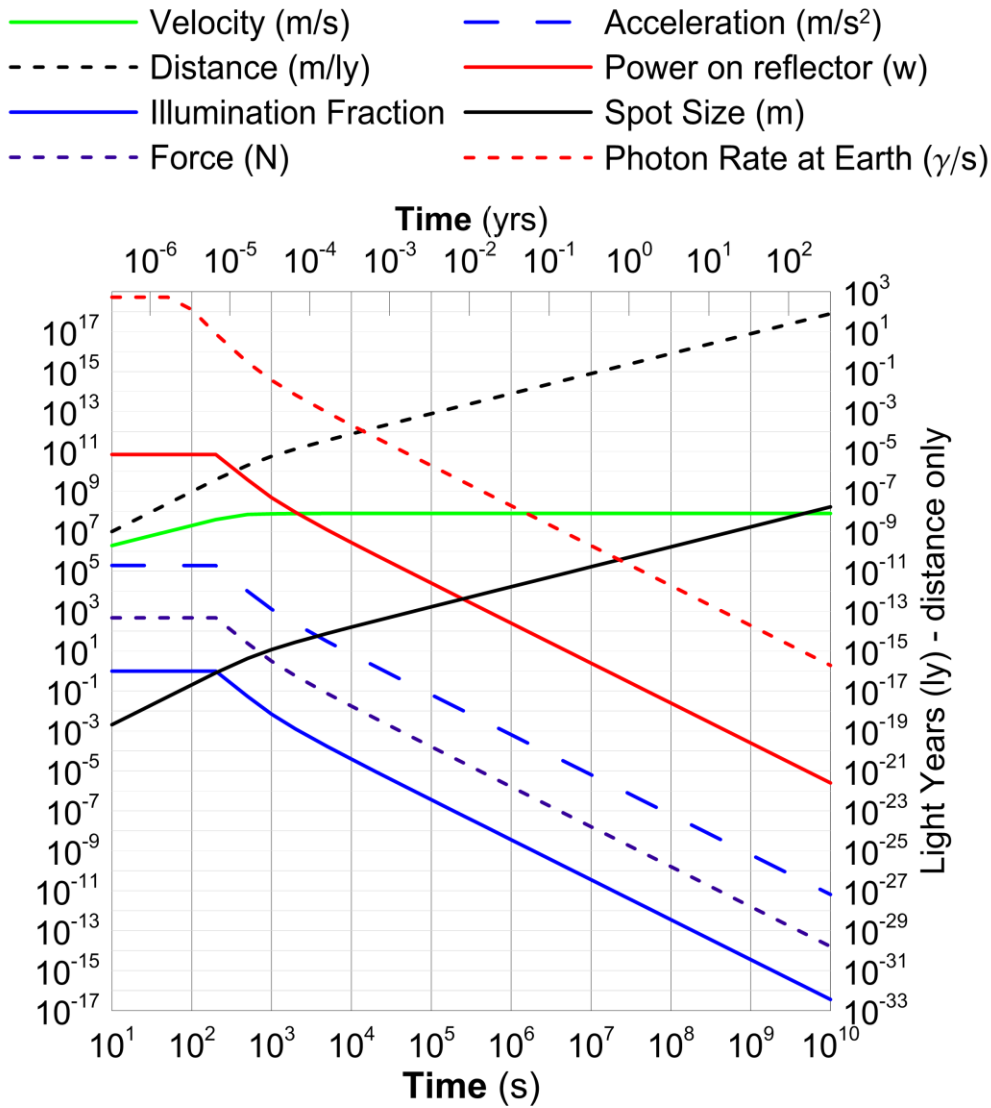


Figure 13 - Parameters for full class 4 system with wafer SC and 1 m sail. Craft achieves 26% c in about 10 min and takes about 20 years to get to Alpha Centauri. Communications rate assumes class 4 drive array is also used for reception with a 1 watt short burst from a 100 mm wafer SC. Here the only optical system on the spacecraft is assumed to be the 100 mm wafer. No external optics is assumed.

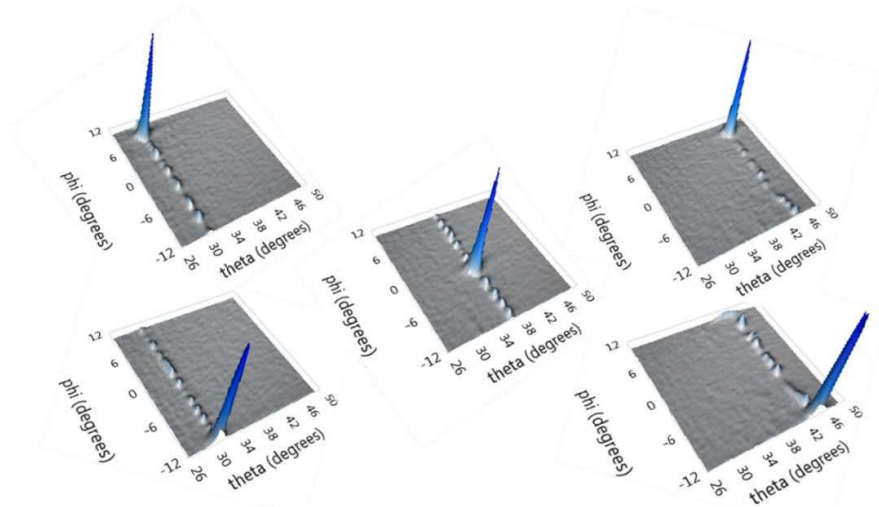


Figure 14 - UCSB Phased array for chip level laser communication with no external optics showing electronic beam steering. Hulme *et al.*, 2014. Another option we are considering is a single laser with a MEMS steering combined with a thin film optic. While not as elegant as a wafer scale phased array it is far simpler in some ways but lacks the full 2D nature of the wafer phased array. The thin film optic in this case adds complexity. Though extremely low mass it must be deployed after launch. More work is needed on these trade studies.

Using the reflector for laser communications would also help greatly. We have NOT assumed this in the link margin calculations. There are many challenges here and ones that will require considerable effort but the rewards will be used in not only interstellar probes but also planetary, space and terrestrial remote sensing, medical, security, *etc.* The list of possible uses for self-contained autonomous system is endless.

Laser Sail. The laser sail is both similar to and fundamentally different than a solar sail. For small sails, even with low powers the flux can easily exceed 100 MW/m^2 or 10^5 Suns. This requires a very different approach to the sail design. Fortunately the laser line is very narrow so we can tune the laser sail reflectivity to be extremely high and the absorption to be extremely low using multi layer dielectric coatings. The relativistic aspects of the highest speed missions present another problem as the laser wavelength is shifted at the reflector. Laser coatings on glass already can achieve 99.999% reflectivity or absorption of less than 10^{-5} . We have started working with industrial partners and have designed a "roll to roll" process that is a multi-layer dielectric on plastic that achieves 99.995% reflectivity (in design). This looks good enough for most cases except the extreme flux of the true interstellar probes which use small (~1 m size) reflectors. For the small reflectors we propose using a pure dielectric reflection coating on ultra-thin glass or other material. Spherical (bubbles) sails are an option for testing. The loss in fiber optic quality glasses allows loss in the $\text{ppt}(10^{-12})/\mu\text{m}$ (of thickness) which is even better than we need. This is an area we need to explore much more. The flux at the tip of high power single mode fiber optic exceeds 10 TW/m^2 , higher than we need. Rather than the typical 1/4 reduced wavelength anti reflective (AR) dielectric coating, we will need to design a 1/2 wave reflection coating for the sail. The scaling of flux on the reflector is:

$$\text{Flux} = P_0 / D^2 \quad \text{Assume optimized case where sail mass} = \text{payload mass } m_0 = m_{\text{sail}} = D^2 h \rho$$

$$D = (m_0 / h \rho)^{1/2} \quad \rightarrow \text{Flux} = P_0 / D^2 = P_0 h \rho / m_0$$

Note the flux is proportional to the thickness and density (smaller sail) and inversely proportional to the mass (larger sail). This means lower mass payloads have high flux requirements on the sail. We will analyze additional reflector requirements and work with industry and the solar sail community.

We consider two cases below. One where light is either reflected or absorbed but none is transmitted through the sail (appropriate to dielectric and metal coatings) and two where some light is transmitted through the reflector (appropriate to dielectric only coatings).

$$P = \frac{P_0}{\gamma} = \text{power at reflector (freq of photons reduced by } \gamma)$$

$$P_0 = \text{Laser power that is initially transmitted}$$

1) **Case of NO transmission thru reflector - all is reflected or absorbed**

$$F = \frac{dp}{dt} = \frac{2P\varepsilon_r}{c} + \frac{P(1-\varepsilon_r)}{c} = \frac{P(1+\varepsilon_r)}{c}$$

P = Laser power at reflector
 ε_r = Reflector reflection coef
 $\varepsilon_r = 1$ for perfect reflection
 $\varepsilon_r = 0$ for perfect absorption

2) **Case of some transmission of light thru reflector**

$$F = \frac{dp}{dt} = \frac{2P_r}{c} + \frac{P_A}{c} = \frac{P}{c} (2\varepsilon_r + (1-\varepsilon_r)\alpha)$$

α = absorption coefficient

IF $\alpha = 1$ (complete absorption inside reflector of the part not reflected)

$$\text{Then: } F = \frac{dp}{dt} = \frac{P}{c} (2\varepsilon_r + (1-\varepsilon_r)) = \frac{P(1+\varepsilon_r)}{c} \text{ as case 1)}$$

P = Laser power at reflector

P_r = Laser power reflected at first surface = $P\varepsilon_r$

P_A = Laser power absorbed inside reflector = $P(1-\varepsilon_r)\alpha$

P_T = Laser power transmitted thru reflector = $P - P_r - P_A$

$P = P_r + P_A + P_T$

ε_r = reflector reflection coef

$\varepsilon_r = 1$ for perfect reflection

$\varepsilon_r = 0$ for no reflection

$\alpha = 0$ for no absorption of light inside reflector

$\alpha = 1$ for complete absorption of light inside reflector (ie no transmission)

Reflector Mass - Current reflectors have thicknesses in the 1-10 μm range. Future technologies may allow us to greatly reduce this and thus extend the speed and distance of our probes. In this paper we assume current technologies for reflectors with some modest improvements. It is important to consider

the implications of future advances in this area. Recall the (non relativistic) scaling of speed for the case

$$\text{of reflector mass} = \text{spacecraft mass } m_0 : v_{\text{max} \rightarrow \infty} = \left(\frac{2P_0 d}{c \lambda} \right)^{1/2} (h \rho m_0)^{-1/4}$$

The scaling of speed with the thickness of the sail "h" $v_{\text{max} \rightarrow \infty} \propto (h \rho m_0)^{-1/4}$ means that as the sail thickness decreases the speed will increase.

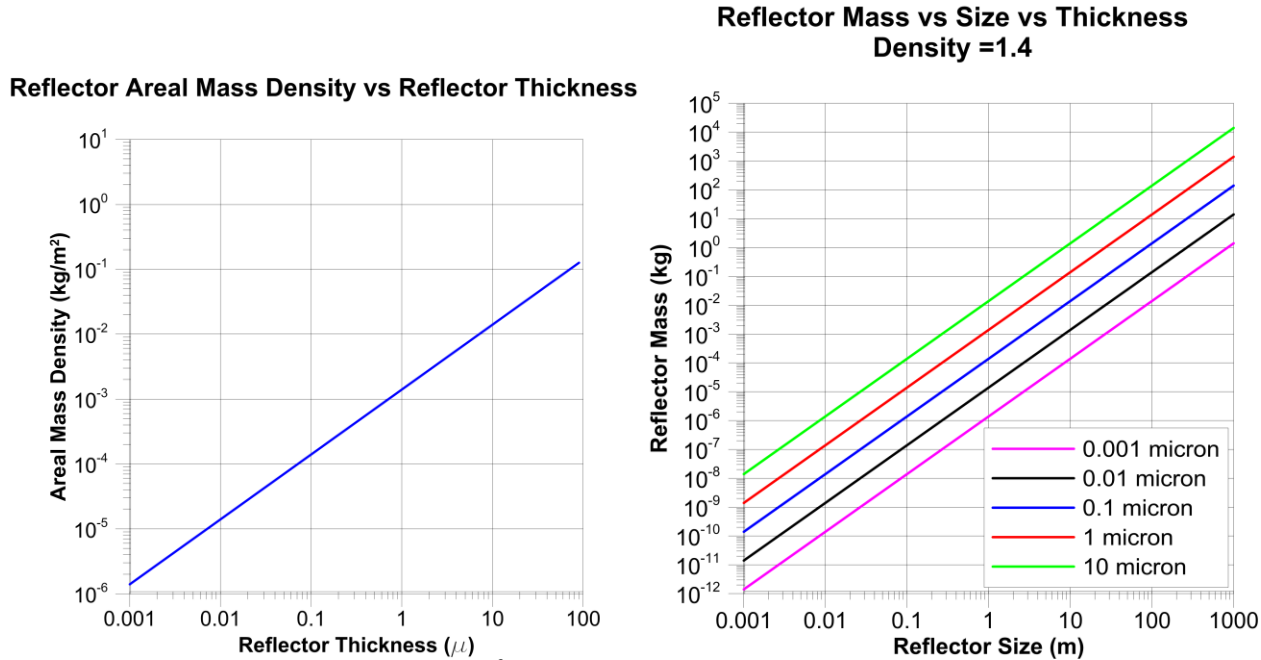


Figure 15 – Left – Reflector areal mass (kg/m³) vs reflector thickness for density =1.4 g/cc typical for plastic. Glass films would have a density about 1.8 times larger. Right – Mass of the reflector vs size (assumed to be square) vs reflector thickness. Current reflectors are between 1 (cutting edge) and 10 (conservative) microns thick. Future technologies may allow us to make significantly thinner reflectors. A part of our roadmap to reduce the reflector mass, though we assume in our system analysis a 1 micron thick reflector. Note that the final speed only depends on the system mass to the inverse ¼ power (m^{-1/4}) for the case of payload mass equaling reflector mass. Hence increasing the reflector thickness has only a mild effect on the speed.

Multi layer dielectric on metalized plastic film - Metalized thin film plastic films with multi layer dielectric coatings can achieve very high reflectivity. In collaboration with industry we have designed a 99.995% reflective system suitable for large scale "roll to roll" production. Note the reflectivity is tuned to the narrow laser line and that these reflectors are NOT suitable for solar sails which use the broad spectrum of the sunlight to propel them. We illustrate this below with a putative design for our Yb baseline 1064 nm laser case. For large sails (>10 m diameter) this is a suitable choice. For example a 30 meter square sail on 10 μm thick plastic film will have a mass about 13 kg while a more advanced thin film of 1 μm thickness would have a mass of about 1.3 kg.

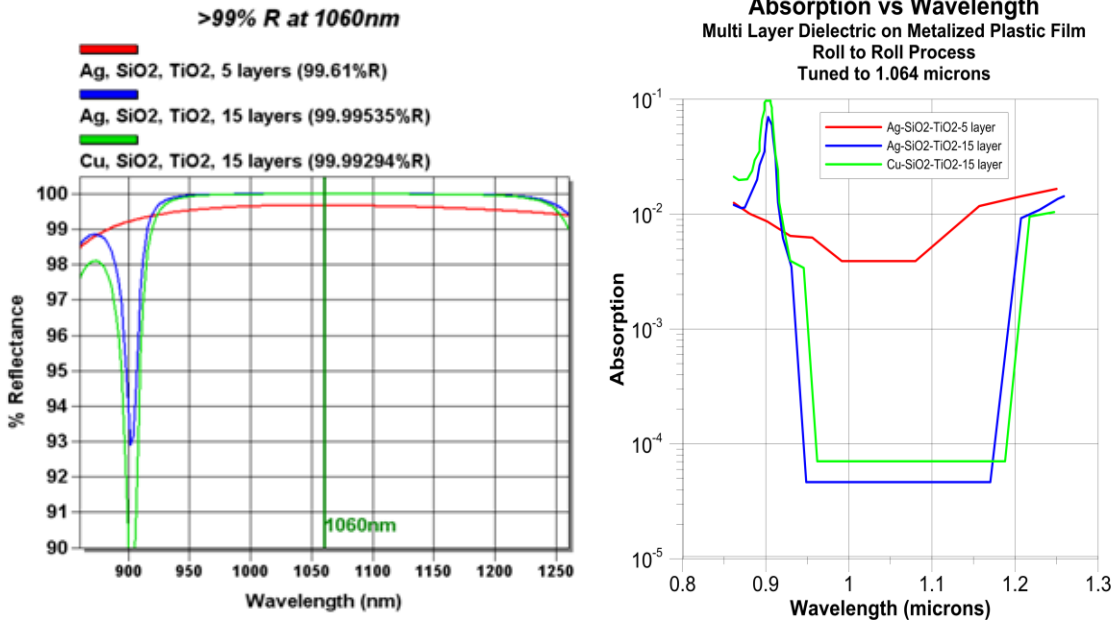


Figure 16 – Multilayer dielectric deposited on metalized plastic film. The reflectivity is tuned to be maximum at the laser wavelength. Left – Reflectivity vs wavelength for several models of the reflector with varying dielectric layers and compositions. Right – Same but absorption is plotted. Note minimum at the laser wavelength of 1.06 microns with an absorption of about 50 ppm. This reflector was designed to be part of a mass production “roll to roll” process applicable to very large reflectors. For our smaller “WaferSat” missions the reflector is relatively small in diameter (meter scale) and hence a roll to roll process is not needed. Roll to roll processing is needed for larger payload masses, which require larger reflectors.

Multi layer dielectric on metalized glass - The use of tuned multi layer dielectric films on metalized glass substrates currently achieves reflections of "five 9's" or 99.999% . The means absorption of less than 10 ppm (parts per million). This is shown for the case of our Yb 1064 nm baseline in the figure. Note again that the high reflectivity is tuned to the narrow laser line. We note that even better performance has been achieved for the 30 cm LIGO multi layer dielectric on glass mirrors with about 0.5 ppm absorption. In this case the mirror does not have metal coatings but the mirrors are quite thick (multiple cm thick).

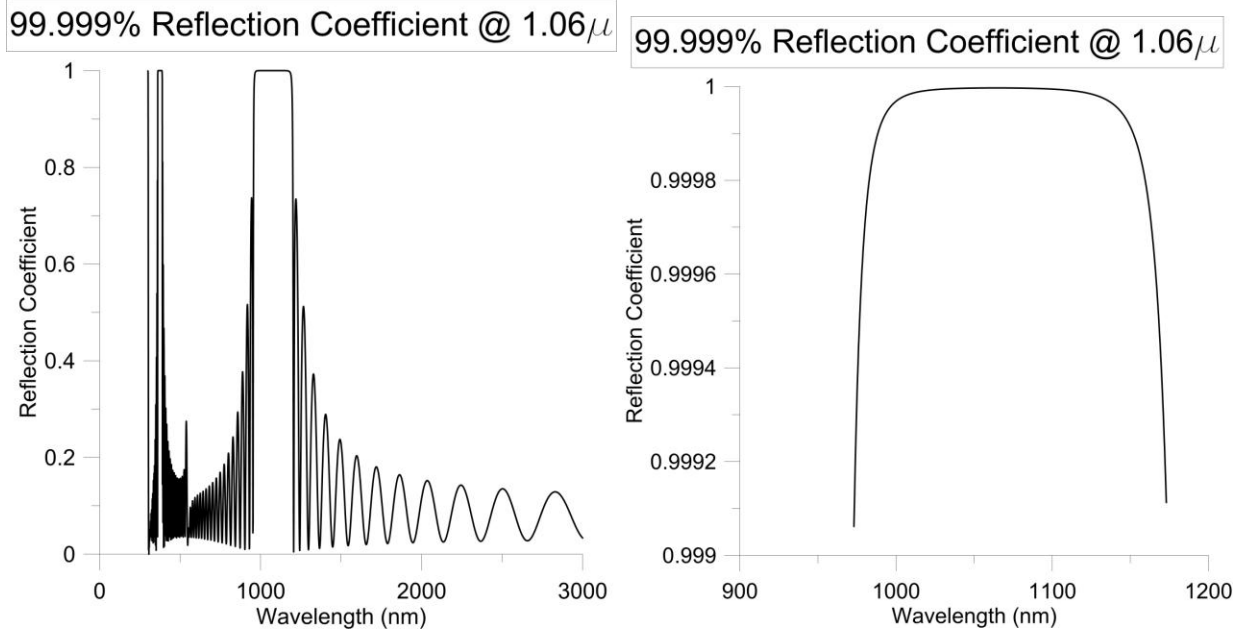


Figure 17 - Multilayer dielectric deposited on metalized glass film. The reflectivity is tuned to be maximum at the laser wavelength. Left – Reflectivity vs wavelength over a large wavelength range showing the tuning of maximum reflection at the laser line. It is thus possible to design a reflector that is extremely reflective at the laser wavelength but highly absorptive at longer wavelengths and thus good as a thermal radiator (extreme example of a “selective coating”. Right – Same but over the narrow region near the laser line (1064 nm). This corresponds to an absorption of about 10 ppm. For thin glass films this could be adopted to a roll to roll process if needed for large reflectors, though it not currently designed this way.

Multi layer dielectric on glass with no metal - For very high flux sails, such as the small relativistic WaferSat probes, the flux on the reflector becomes so large that metalized reflectors, even with multi layer dielectric coatings become extremely difficult to make. The issue is that the metalized sub structure is not reflective enough so the thermal management becomes a critical problem (sails vaporize). One solution is the remove the metals completely and use a fully dielectric reflector. This is what we propose for the extreme cases of high flux small sails. Glasses designed for fiber optics and other photonic communication applications have extremely low absorption coefficients with ppt (parts per trillion) per micron thickness are currently achieved. While the reflection coefficient will not be as large as it is for the metalized cases in general, they are sufficient. Note in this case the absorption takes place in the bulk of the glass of the reflector and dielectric coating while in the metalized plastic and glass case it is absorption in the metal film that is dominant. We plot the absorption coefficients for modern fiber optic glasses to illustrate this. We note the achieved performance for the 30 cm diameter (40 kg mass) LIGO multi layer dielectric on glass mirrors with about 0.5 ppm absorption. In this case the mirror does not have metal coatings. The mirrors are quite thick (multiple cm thick). As a comparison a 1 cm (10^4 micron thick piece of ZBLAN glass with 20 ppt/ micron absorption coefficient would have a total absorption of $20 \times 10^{-12} \times 10^4 = 2 \times 10^{-7}$ or 0.2 ppm at a wavelength of 1.06 microns.

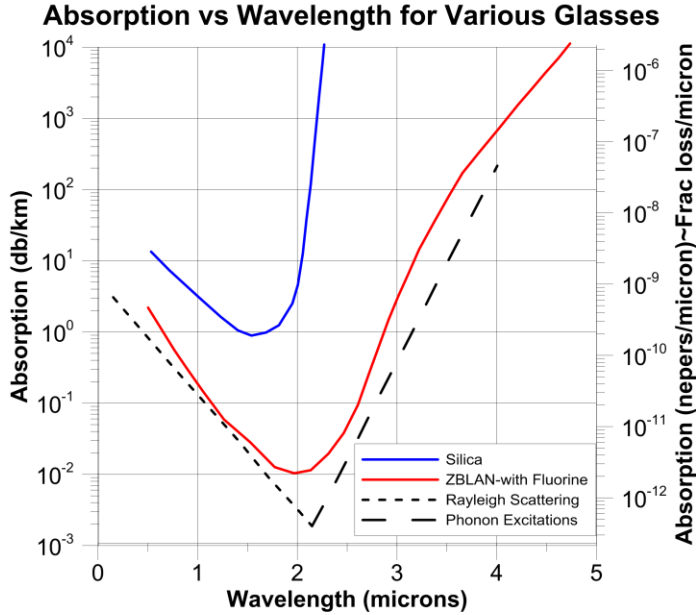


Figure 18 – Absorption for optimized glass designed for fiber optics. This is extremely low OH glass and has excellent performance for extremely high flux applications such as our small reflector relativistic designs require. Note the absorption at our laser wavelength of 1.06 microns is about 20 ppt/ micron reflector thickness. What is not shown is the optimized reflectivity for the multi layer dielectric coating. In this system there are no metal layers which allows us to achieve such low absorption.

Reflector Stability and Shaping - A critical issue will be the stability of the sail. There are a number of perturbative effects. These include laser instabilities and laser mode issues, differential forces on the sail and mechanical modes in the sail, heating of the sail and laser pointing instability.

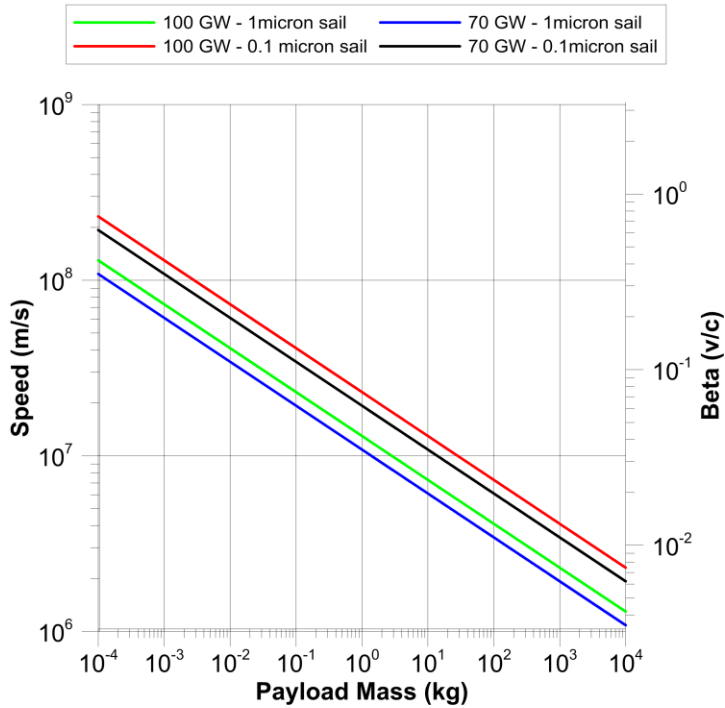
This is a complex sets of issues that requires a significant amount of research and development. This will not be trivial. Some ways to mitigate these issues are spinning the sail (especially if circular) and shaping of the reflector into a slight conic (similar to a reentry vehicle). Feedback from the sail to the laser will help but the time of flight will lower the effective servo bandwidth for this. Ideally a self stabilizing system is desired. We see this as one of the most critical issues to overcome.

Beam Shaping and Sail Stability - Since we are using a phased array to form the target spot we can shape the beam profile by adjusting the phase of the array. Normally we would produce a Gaussian beam pattern but there are other options that would increase sail stability. One is to form a minimum (null) in the middle of the beam which would damp small perturbations and self stabilize the sail.

Effect of reflector thickness - In the future we can anticipate thinner sail materials as increased nanofabrication of ultra thin films become available. Graphene may be one such material that might be possible to coat for good reflectivity. Here we show the effect of using reflectors of varying thickness. Since there speed with continued illumination scales as the sail thickness $h^{-1/4}$ for the optimized case of sail mass = payload mass we show a plot of the effect for a few selected sail thickness.

$$v_{\max-\infty} = \left(\frac{P_0(1 + \epsilon_r)d}{c\lambda} \right)^{1/2} (h\rho m_0)^{-1/4}$$

Speed vs Payload Mass and Sail Thickness
 Optimized for Payload Mass = Sail Mass
 10 km array size



Orbital Trajectory Simulation - We have worked out the orbital trajectories assuming a Sun synchronous LEO based DE-STAR (it can be placed in other orbits) to keep it fully illuminated except during a few eclipses. For the very low mass payloads the time to near maximum speed is so fast that the spacecraft travels in nearly a straight trajectory as the acceleration time is small compared to a LEO orbital time while for the heavier payloads this is not true and the path is more complex (Zhang et al 2015)..

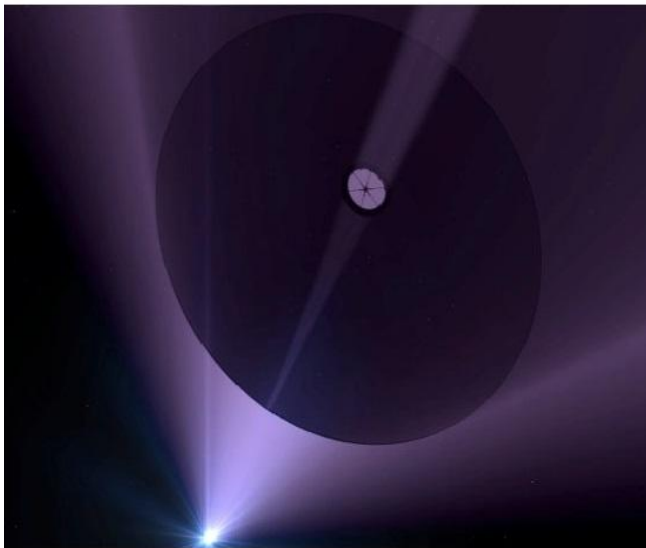
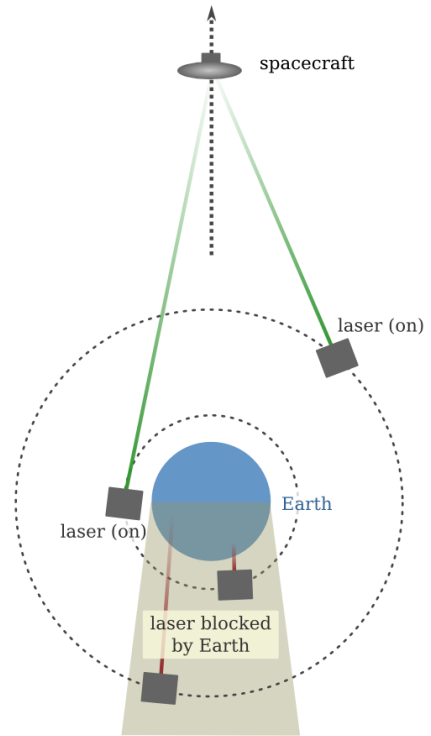
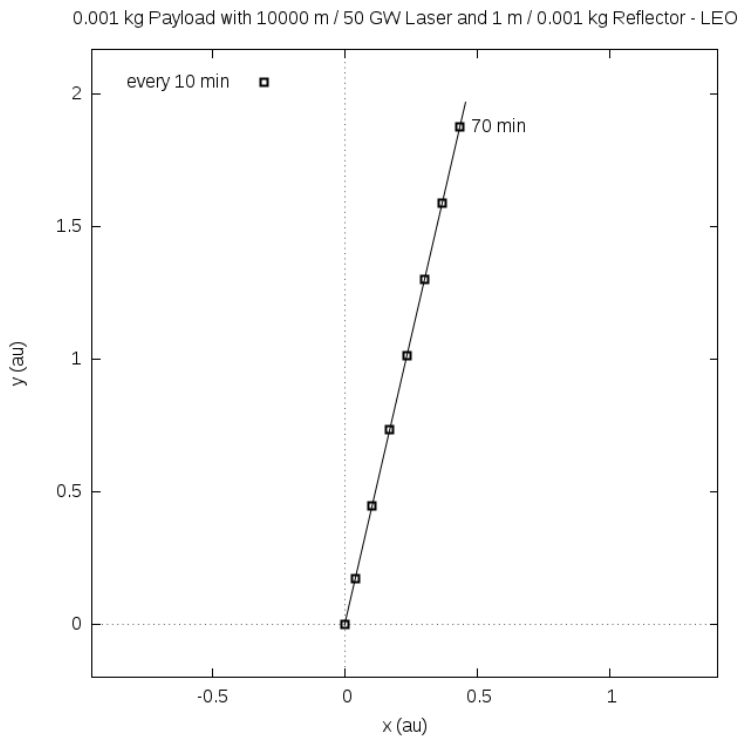


Figure 19 – Artistic rendering of a laser driven reflector.

Multiple Independent Re-entry Vehicles Option - An option to be considered it to use a large number of wafer scale spacecraft contained in a larger (but still relatively low mass) "mothership". Upon entry near the target star the mother ship would eject the wafers which would then interconnect with each

other and the mothership via an optical link. The larger mothership would then transmit the collected data back to Earth. To some extent this precisely mimics the current strategy for planetary probes in our own solar system except we envision several hundred "WaferSats", each with their own power (RTG and PV) as well as their own optical comm and laser attitude control. Each wafer has a mass of about 1 gram and hence a 1 kg mothership could carry perhaps 500 of these and disperse them in a roughly 1AU spacing on a 20x20 array upon entry to allow a much more thorough exploration. Since command and control back to earth is not feasible due to TOF issues the system would have to be autonomous.

Braking to Enter Orbit on Arrival - A very difficult challenge is to slow the spacecraft to typical planetary orbital speeds to enable orbital capture once arriving. This task is extremely difficult as the initial entry speeds are so high ($\sim c$) and the orbital speeds are so low ($\sim 10^{-4} c$). Dissipating this much energy is challenging. We have considered using the stars photon pressure, the stellar wind (assuming it is like our own solar system), using the magnetic coupling to the exo solar system plasma. None of these techniques appears to be obviously able to accomplish this task and much more work and simulation is needed. A simple fly-by mission is clearly the first type of mission to explore in any case to assess the environment in a given system to design (if possible) an optimized braking strategy.

Communications - Another use of the DE-STAR system would be for long range interstellar communications to and from the spacecraft. This is a critical issue for long range interstellar probes in the future. Can we get high speed data back?

DE-STAR to spacecraft data rate - Consider an optical link calculation with DE-STAR 4 which emits about 50 GW at 1.06 μm or about $3 \cdot 10^{29} \gamma/\text{s}$, with a divergence half angle of

$$\theta \approx \frac{\lambda}{D} \approx 10^{-10} \text{ rad} \quad (22)$$

At a distance of $L = 1 \text{ ly}$ ($\sim 10^{16} \text{ m}$) the spot size (diameter) is about $D_s \sim 2 \cdot 10^6 \text{ m}$. For the case of the 100 kg robotic craft and with a 30 m diameter reflector this gives a **spacecraft** received photon rate of $3 \cdot 10^{29} \times (30/2 \cdot 10^6)^2 \sim 7 \cdot 10^{19} \gamma/\text{s}$. If we assume it takes 40 photons per bit (which is very conservative) this yields data rate of about $2 \cdot 10^{18} \text{ bits/s}$, clearly an enormous rate. See figure.

Spacecraft to DE-STAR data rate - Assume the spacecraft has a very modest 10 W transmitter on the spacecraft (an RTG for example) for an optical link at the same basic wavelength $\sim 1.06 \mu\text{m}$ (slightly different to allow full duplex communications if needed) and that it uses the same 30 m reflector as for the photon drive but this time it uses it as the communications transmitter antenna (mirror). We do the same basic analysis as above. 10 W at 1.06 μm or about $5 \cdot 10^{19} \gamma/\text{s}$, with a divergence half angle of

$$\theta \approx \frac{\lambda}{D} \approx 3.5 \times 10^{-8} \text{ rad}$$

At a distance of $L = 1 \text{ ly}$ ($\sim 10^{16} \text{ m}$) the spot size (diameter) is about $D_s \sim 3.5 \cdot 10^8 \text{ m}$. For the case of the 100 kg robotic craft and with a 30 m diameter reflector transmitting BACK to a DE-STAR 4 which acts as the receiver this gives a received (by the DE-STAR) photon rate of $5 \cdot 10^{19} \times (10^4 / 3.5 \cdot 10^8)^2 \sim 4 \cdot 10^{10} \gamma/\text{s}$. If we assume it takes the same 40 photons per bit this yields a **received (at Earth** or wherever the DE-STAR system is located) data rate of about $1 \cdot 10^9 \text{ bits/s}$ or 1 Gbps. At the nearest star (Proxima Centauri) at a distance of about 4 ly the data rate at Earth from the spacecraft is about 70 Mbps. **Live streaming >HD video looks feasible all the way to our nearby interstellar neighbors.** This is summarized in Figure xx.

DE-STAR 4 - 70 Gw

Reflectivity: 1
 Reflector diam: 30 m
 Wavelength: 1.06 μm

Spacecraft xmit and rcv:
 Dish size: 30 m
 Power: 10 w
 Wavelength: 1.06 μm
 Photon/bit : 40

- Power on reflector (w)
- DE-STAR Photons/s
- Photon flux at spacecraft (ph/m²-s)
- Photons per sec on spacecraft receive dish
- Bits/sec received by spacecraft (bits/s)
- Spacecraft transmitted beam divergence - full angle (rad)
- Spacecraft transmitted spot size at DE-STAR (m)
- Spacecraft transmitted flux at DE-STAR (w/m²)
- Photon flux at DE-STAR from spacecraft (photons/m²-s)
- Photon rate received by DE-STAR (ph/s)
- Bit/s received by DE-STAR from spacecraft (bits/s)

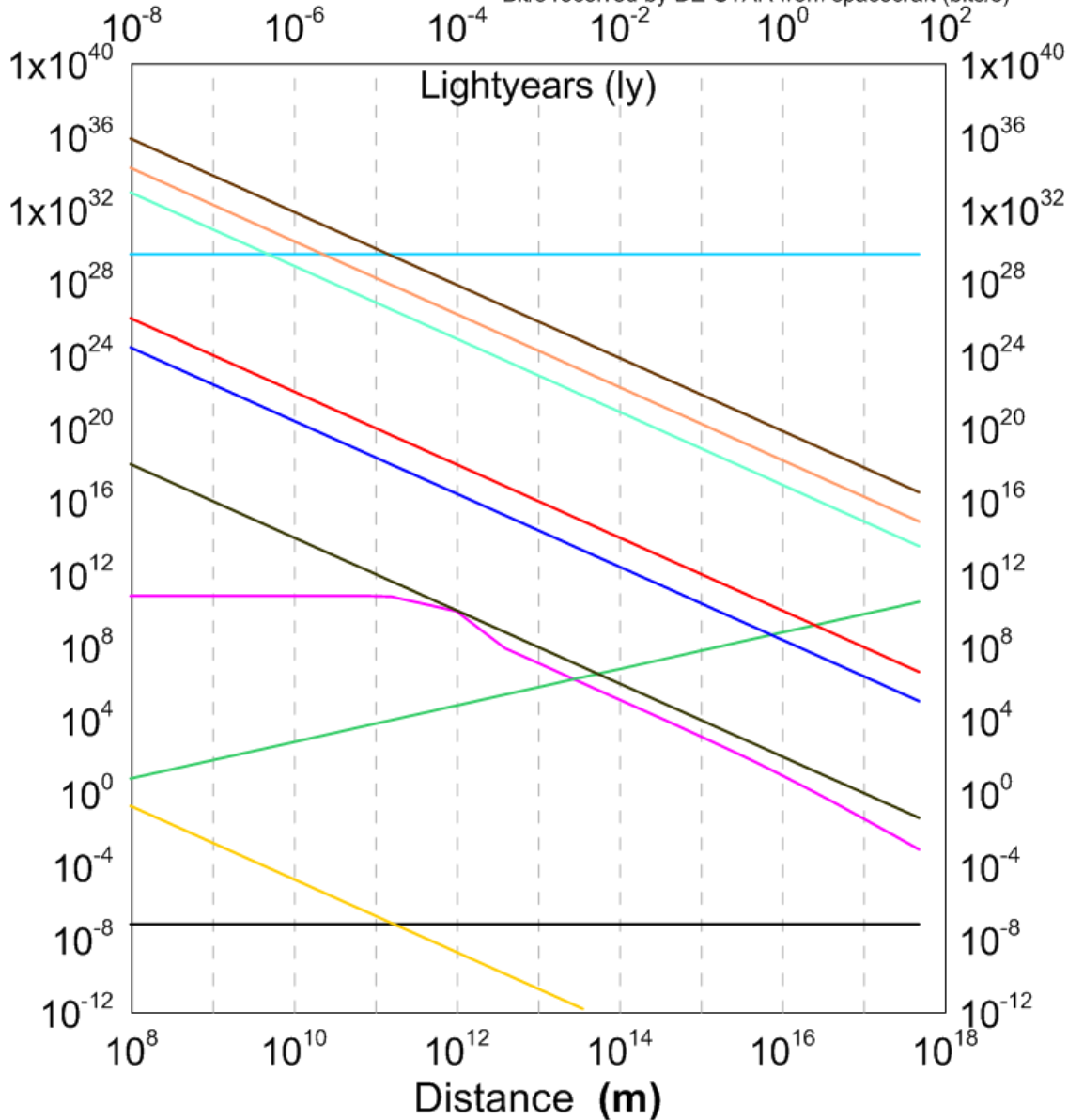


Figure 20 – Flight parameters including data rates for a 100 kg spacecraft with a conservative 30m sized reflector made from the “roll to roll” multi layer dielectric process as described above. Laser driver is 10 km (DE-STAR 4) array with an optical output of 70 GW power.

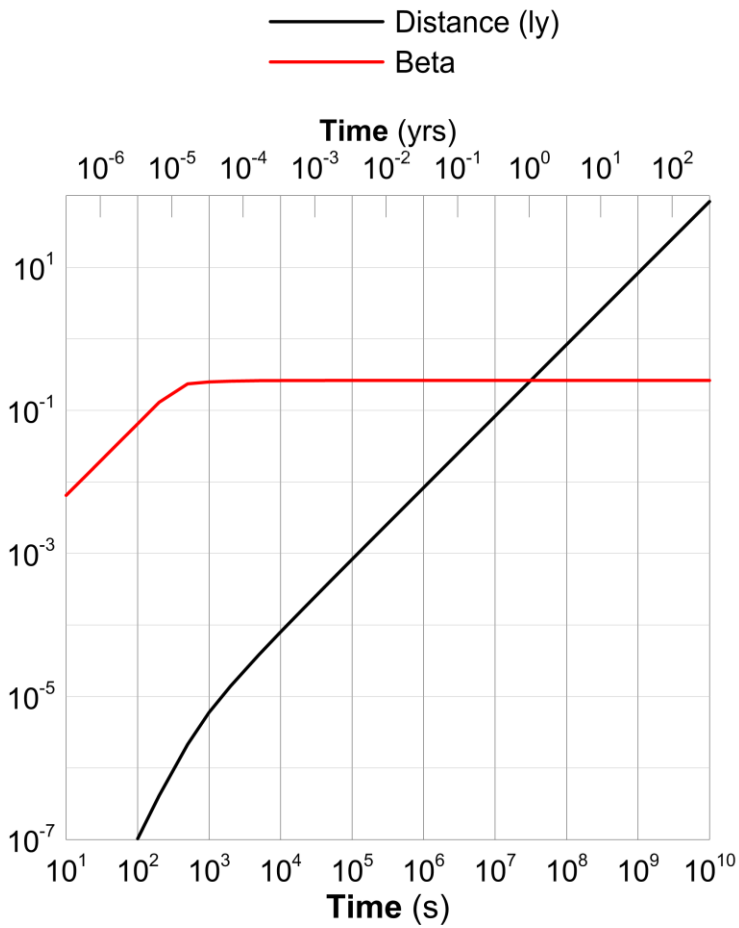


Figure 21 – WaferSat case with same DE-STAR 4 driver (70 GW – 10 km array) as in Fig 20 but for wafer scale spacecraft driven by 1 meter sized reflector (1 micron thick), Wafer mass is 1 g and reflector mass is 1.4 g. Total mass is 2.4g. Parameters shown are relativistic factor beta and distance vs time. Note that Alpha Centauri (4.3 ly) is achieved in about 15 years with 10 ly achieved in about 35 years.

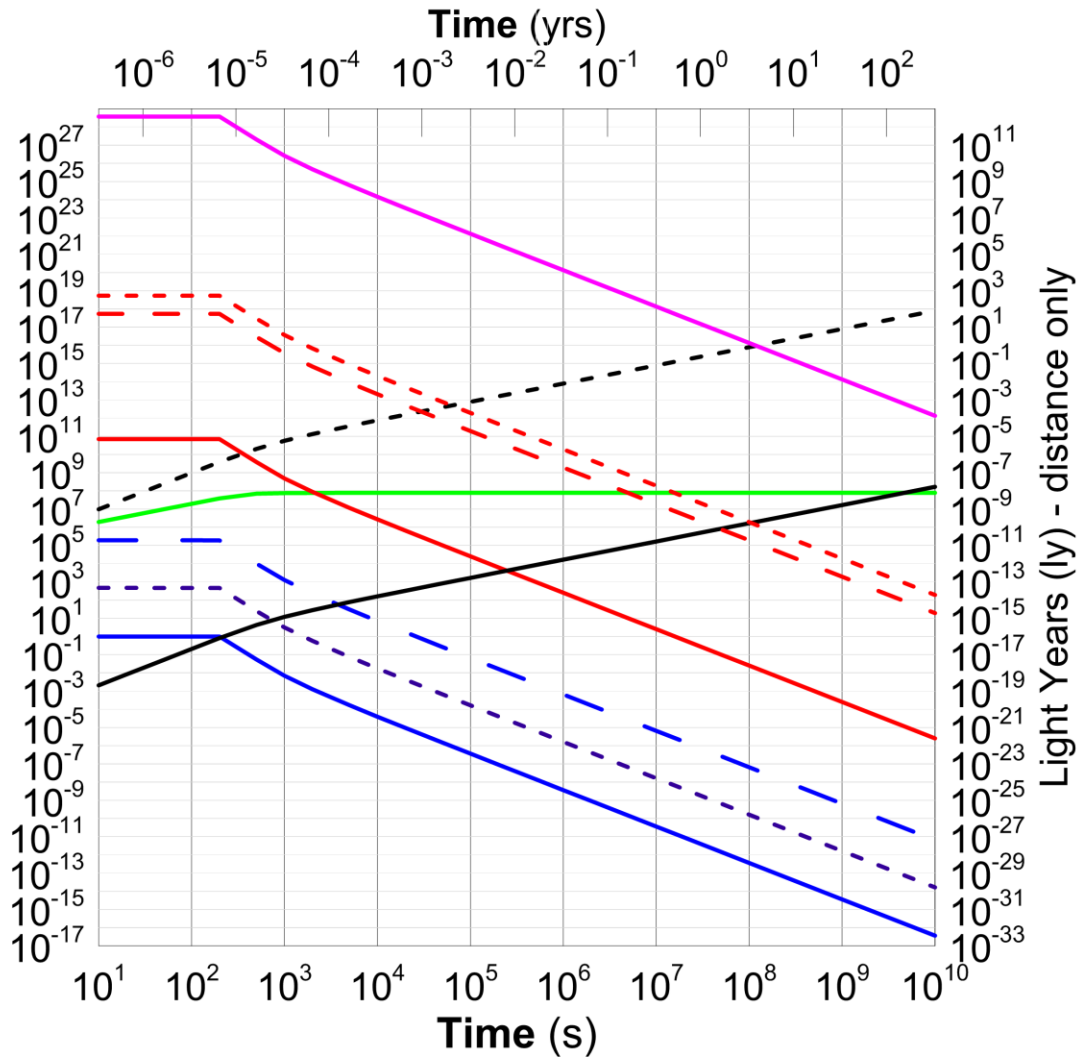
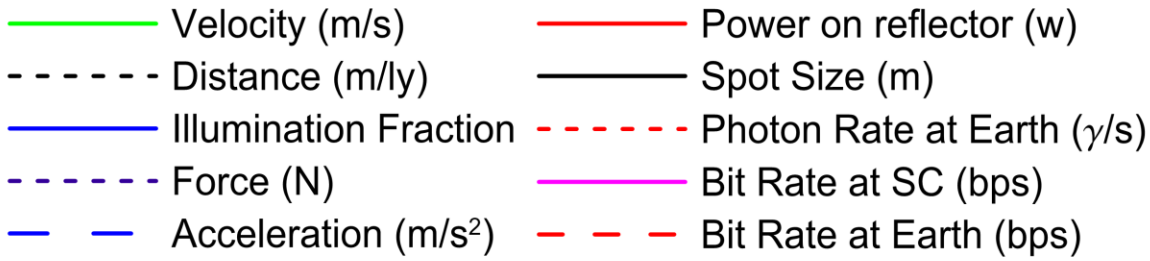


Figure 22 - Parameters for full class 4 system with wafer SC and 1 m sail. Craft achieves 26% c in about 10 min and takes about 20 years to get to Alpha Centauri. Communications rate assumes class 4 drive array is also used for reception with a 1 watt short burst from a 100 mm wafer SC. Here we use the 1 meter drive reflector as the transmit and receive optical system on the spacecraft. In the previous figure for the same wafer scale spacecraft the **only optical system on the spacecraft was the 100 mm wafer**. The data rate received at the Earth at Alpha Centauri is about 8 kbs assuming we can use the DE-STAR 4 driver as the receiver.

Backgrounds - The relevant backgrounds at 1 μm wavelengths are optical emission from the telescope/array, zodiacal emission from our solar system dust both scattering sunlight and emitting thermal

radiation (Zodi) and the Cosmic Infrared Background (CIB). It is assumed that the latter is the sum of all unresolved galaxies in the universe in the field of view. The Cosmic Microwave Background (CMB) is not relevant and light from our galaxy is relatively small unless looking directly at a star. If searches/communications are done inside our atmosphere then the situation is more complex due to emission from our atmosphere. For communications and for SETI programs we are looking at intelligently modulated signals not just random noise.

The Zodiacal light is highly anisotropic and also time dependent and location of the Earth in the orbit around the sun dependent. We treat this from data collected from the DIRBE instrument on COBE. The CIB is far more isotropic on modest angular scales and becomes largely point like on very small scales. Again we model this from the DIRBE data on COBE and subsequent measurements. We also model the optics at various temperatures and the Earths atmospheric emission for inside the atmosphere measurement but will focus here on orbital programs. The Zodi and CIB are shown in Fig. 13 and Fig. 14.

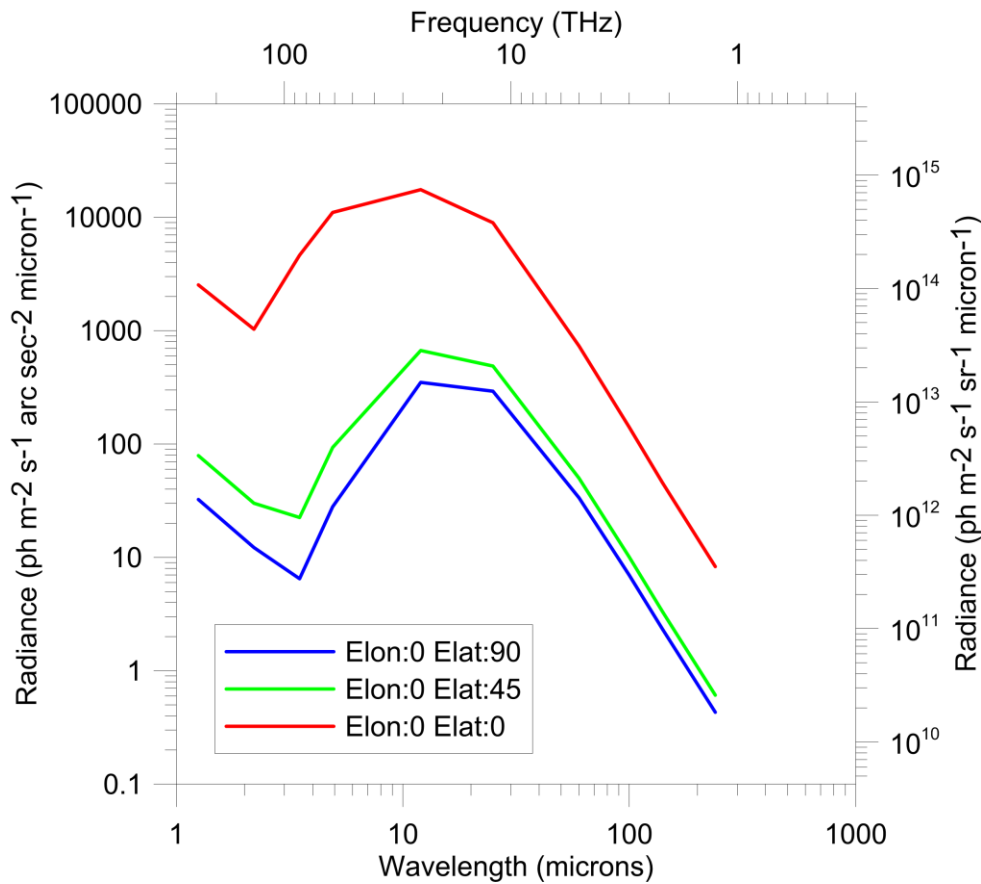


Figure 23 - Zodiacal emission from the COBE DIRBE measurements showing day 100 of the COBE mission at observation from the along the ecliptic plane to 45° to 90° (ecliptic pole). William Reach private communication (2012). Note the radiated peak from solar system dust around 15 μm due to the dust temperature being about 200 K and the scattered rise near 1 μm due to the zodi dust scattered sunlight.

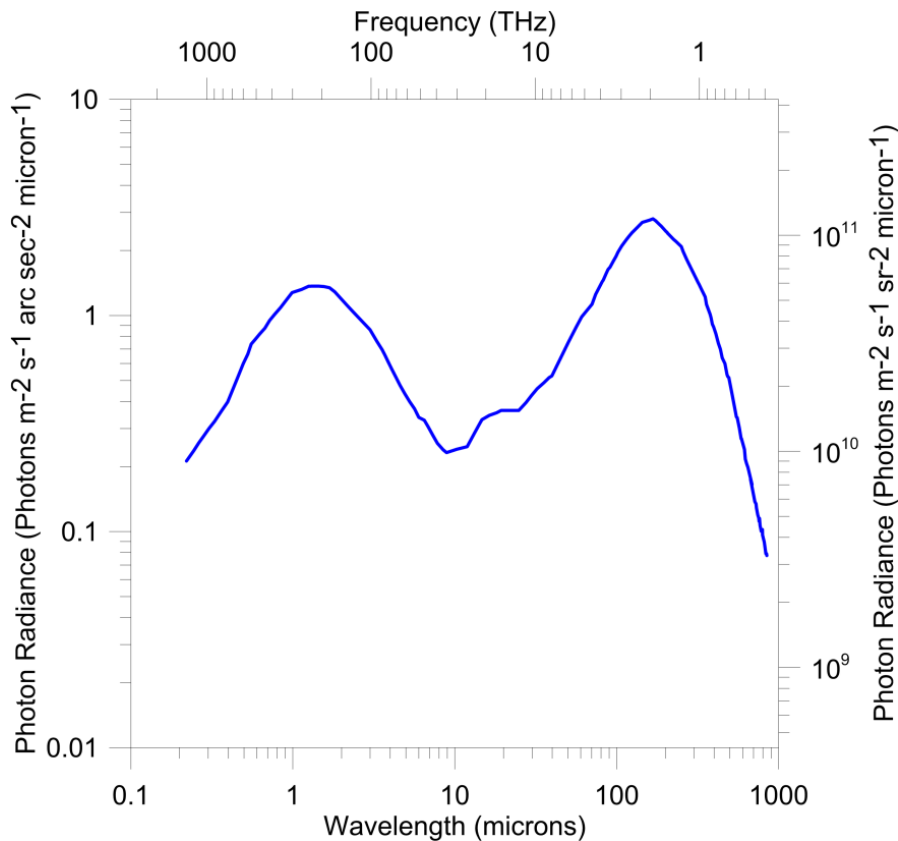


Figure 24 - Cosmic Infrared Background (CIB) radiation from COBE DIRBE and subsequent measurements.

Implications of the technology to SETI - The same laser used to drive the probe can also be used as a beacon to "signal" other planetary systems as well as establish extremely long range "communications" systems with data delays modulo the speed of light. We discuss this in detail in detail in Lubin et al 2015 (JBIS) and Lubin 2016 (JBIS). The implications for SETI searches are quite profound. A similarly "advanced" civilization like ours would be visible across the entire visible universe (horizon) if two DE-STAR 4 units were to face each other. This implies that optical SETI searches can not only search nearby planetary systems but could search the entire universe for similar or more advanced civilizations. If the current Kepler statistics ($\sim 1/4$ of stars having planets) on the abundance of suitable planets is scalable to the entire universe, this would imply of order 10^{20} planets within our horizon. We show in Lubin 2016 that even ground based searches using modest existing apertures can detect civilization with technology at our current level (though we have not deployed it yet) at relatively high redshift. Pondering the number of possible planets this allows us to search for has profound implications.

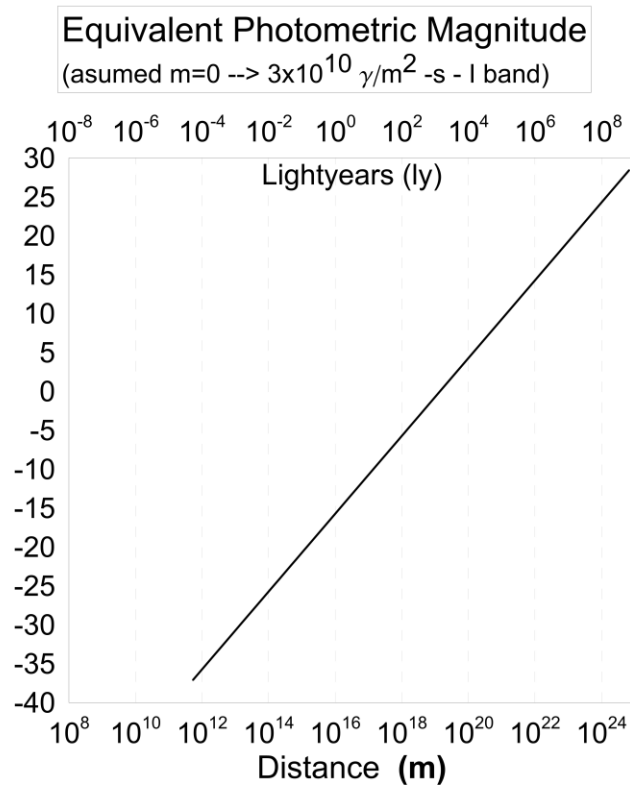


Figure 25 – Equivalent I band photometric magnitude of DE-STAR laser driver as observed vs distance of observation. Even at 1 Gly the laser driver would be visible in a modest telescope by another civilization. Note that this is the equivalent photometric magnitude which uses a broadband filter ($R \sim 3$) and that an optimally tuned filter would have vastly better SNR as it would block the background light. We assume a worst case of an I band photometric filter. Even with this extremely pessimistic design the laser driver is visible across the entire horizon.

**DE-STAR 4 - 50 Gw
Out to 1 Gly**

- DE-STAR Photons/s
- Spacecraft transmitted spot size at DE-STAR (m)
- Spacecraft transmitted flux at DE-STAR (w/m²)
- Photon flux at DE-STAR from spacecraft (photons/m²-s)
- Photon rate received by DE-STAR (ph/s)
- Bit/s received by DE-STAR from spacecraft (bits/s)

Wavelength: 1.06 μm
Photon/bit : 40

~2 Mbs @ 1 Gly
Detectable across universe

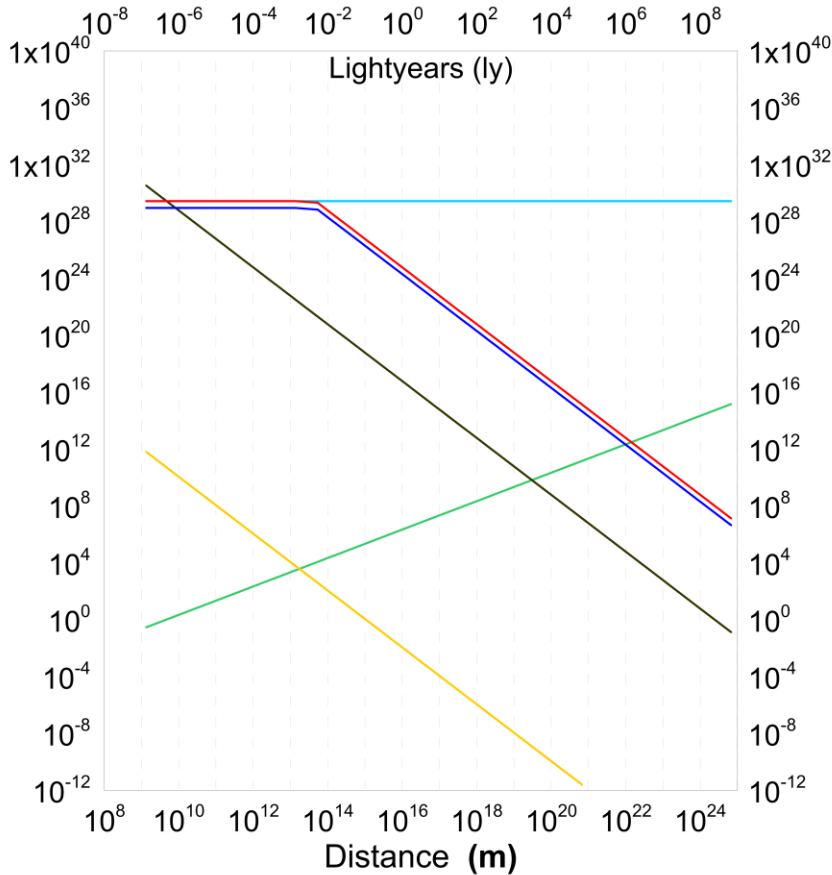


Figure 26 – Photon and data rate for two civilizations with comparable DE-STAR 4 systems facing each other with an optimally tuned filter (resolution bandwidth to laser to minimize background) where each unit is used both for transmission and reception. Even at 1 Gly distances data rates are high.

Interstellar and Interplanetary Dust Impacts – The issue of dust grain and gas (molecular and atomic) as well as electron and proton impacts with a relativistic craft are important.

We will consider interstellar and interplanetary impacts separately. The latter is only important during the acceleration phase but may also be indicative of the dust impacts upon arrival at a distant solar system, though the interplanetary dust around other stars is poorly understood currently.

Interstellar dust – Interstellar dust is estimated to exist over a very large range of sizes from a few molecules to around 100 nm in size. A small fraction is thought to consist of larger refractory material that condensed as the material left the stars. The dust density in the local interstellar medium of the Local Bubble is estimated to be approximately 10^{-6} grains/m³. For a dust grain of 100 nm in size the mass is of approximately 10^{-18} to 10^{-17} kg.

The total number of hits during the journey on the spacecraft is given by:

N (hit rate during journey of length L) = $n \sigma L$ = n (# density #/m³) * σ (cross section of craft (this dominates over the small dust/ gas cross section) * L (journey length (m)).

Assuming $n = 10^{-6}$ dust grains/m³ and $L = 4 \times 10^{16}$ m (~ 4 ly – distance to α -Centauri)

$n * L = 4 \times 10^{10}$ (# grains/m² during the journey). This is a large number and thus we see that the number of grain hits during an interstellar journey is not small. However we have some control over the spacecraft effective cross section (σ) as well as shielding if needed.

The cross section can be controlled to some extent. We assume an effective 10x10cm spacecraft.

If we orient the spacecraft “face on – worst case) then $\sigma \sim 0.01$ m² (10 cm wafer)

If we orient the spacecraft “edge on” with wafer thickness = 100 microns (default) then $\sigma = 10^{-5}$ m²

If we use a long and thin wire (difficult but possible) with a 10 micron thick wire then $\sigma = 10^{-10}$ m²

Taking these cross sections we can compute the number of hits during the journey:

Face on - $\sigma = \sigma \sim 0.01$ m ² :	$N = 4 \times 10^8$
Edge on (100 micron thick wafer) - $\sigma = 10^{-5}$ m ² :	$N = 4 \times 10^5$
Long thin rod or wire (10 micron square) - $\sigma = 10^{-10}$ m ² :	$N = 4$

The uncertainties are large and the factor of "4" is meaningless here. We want to get a rough order of magnitude. One question to be answered of course is “what is the consequence of a dust grain hit?”. This is one of the items to test and assess in the roadmap.

Impact energy

The energy per impact for $v = 0.3c$ (10^8 m/s) for a mass $m_{\text{grain}} = 10^{-17}$ kg dust grain (~ 0.1-1 micron sized depending on structure) is $KE_I = m_{\text{grain}} * v^2 / 2 \sim 0.1J$

Total energy deposition of all grain impacts = $KE_T = N * KE_I$

The worst case is the face on case $N = 4 \times 10^8$ $KE_T = 4 \times 10^8 * 0.1J = 4 \times 10^7 J$

Compare this to the total KE of the wafer spacecraft $KE_{sc} = \frac{1}{2} m_{\text{wafer}} v^2 \sim 10^{-3} (kg) * (10^8)^2 = 10^{13} J$

Thus the ratio of the total dust grain KE to the spacecraft KE is:

$KE_T / KE_{sc} \sim 4 \times 10^7 / 10^{13} = 4 \times 10^{-6} \sim 10^{-5}$.

Hence the total energy of impacts is negligible compared to the total KE of the wafer. It is NOT negligible in total energy delivered to the wafer (ie damage to wafer) but it is not all delivered at once and the face on case is the worst case.

Momentum transfer

The total momentum transfer P_T of the dust grains to the spacecraft (assume worst case of an elastic collision which is clearly an over estimate) = $P_T = N * P_{\text{grain}}$

Where the momentum transfer per grain hit is $P_{\text{grain}} = 2 m_{\text{grain}} v$ (=c/3 here) – assuming elastic collision

For a dust mass of $m_{\text{grain}} \sim 10^{-17}$ kg then $P_{\text{grain}} = 2 * 10^{-17} * 10^8 = 2 \times 10^{-9}$ N-s.

Worst case is face on where $N = 4 \times 10^8$ and thus $P_T \sim 4 \times 10^8 * 2 \times 10^{-9} \text{ N-s} \sim 1 \text{ N-s}$

Compare to total momentum of the spacecraft, assuming the worst case of the low mass wafersat) $P_{sc} = m_{sc} * v (=c/3 \text{ here}) \sim 10^{-3} \text{ (kg)} * 10^8 \text{ (m/s)} = 10^5 \text{ N-s}$.

Thus the ratio of the (worst case – face on and elastic collision) momentum dust grain transfer to the spacecraft momentum is:

$$P_T / P_{sc} = 1/10^5 = 10^{-5}.$$

Hence the total momentum transfer of the dust grains P_T to the spacecraft (even for wafers) is negligible.

We need to do much more refined studies/ simulations of the impact of dust grains on the wafer electronics. For example what happens during an impact? Can we build redundant electronics so that dust hits do not compromise the system. If we just blow a hole thru the wafer it is much less problematic than complete shattering. We discuss mitigation and shielding below.

Interplanetary dust

The solar system density and size distribution is more of a concern during the initial drive phase. Dust in the solar system is observed as zodiacal scattering and emission and has been studied in a number of ways, primarily in the infrared. The solar system dust cloud forms a “pancake” shaped cloud in the ecliptic plane. The dust grains are thought to span a range of size with many between 10 and 300 microns. The overall distribution of the smaller sizes is not well known. Mass of the grain is thought to be on average around 150 micro-grams. The density is highly dependent on the location in the solar system is high anisotropic as well as highly inhomogeneous. This makes statements on density imprecise but we can get a rough estimate from modeling the zodiacal light. Using this we get a distance between (larger) dust grains of roughly 10km or a number density of about $10^{-12} / \text{m}^3$. This density is quite low but we lack good information on the smaller dust grains.

Hitting a 1 mm dust grain in the solar system would likely be catastrophic to the local area affected. However going out perpendicular to the ecliptic plane is only $L \sim 0.1 \text{ AU} \sim 10^{10} \text{ m}$ so the total number of impacts would be down about 10^6 compared to the interstellar case from distance alone. The solar system larger dust grains have a lower density $10^{-12} / \text{m}^3$ (compared to the smaller interstellar dust grain density of $10^{-6} / \text{m}^3$) and thus the total number of solar system hits for the larger solar system grains would be very low on average. Of course since the solar system is extremely anisotropic and inhomogeneous the path of the spacecraft will be important in estimating the hit probability.

Dust Impact Rate – The dust impact rate is R (hit rate #/s) = $n \sigma v$ where v is the spacecraft speed.

Assuming $n = 10^{-6} \text{ dust grains/m}^3$ and $v = 0.3c$ (10^8 m/s) we get $n*v = 100 / \text{m}^2\text{-s}$

For the three cases of the wafersat considered above we get rates of:

Face on - $\sigma = \sigma \sim 0.01 \text{ m}^2$:	$R = 1 \text{ Hz}$
Edge on (100 micron thick wafer) - $\sigma = 10^{-5} \text{ m}^2$:	$R = 10^{-3} \text{ Hz}$
Long thin rod or wire (10 micron square) - $\sigma = 10^{-10} \text{ m}^2$:	$R = 10^{-8} \text{ Hz}$

Dust Impact Mitigation – Several techniques exist to mitigate dust impacts. Mitigation can be from minimizing spacecraft geometry (cross section), shielding (for example a thin Beryllium (Be) shield) and spacecraft topology. As we discussed a long thin spacecraft with small cross section relative to the velocity vector can result in large reductions in the number of hit. Shielding needs to be explored

further. A Be shield that is a few mm thick may allow significant protection but this would dominate the mass of the lightest spacecraft (wafersat) significantly. Another solution may lie in a highly redundant topology that allows for a large number of hits and still maintain functionality. It is critical to prevent shattering of the wafer for the low mass case. A wafer could be produced with a “waffle pattern” with small contiguous regions and thinned or even legs attachments that would prevent shattering of the adjacent sections. This is an area where design, simulation and testing with a dust accelerator (currently only good to 100 km/s) is critical to explore.

Shielded Edge on Design – One possible design that combines shielding with an edge on wafer orientation is to make the outer facing (along the velocity vector) edge out of Be or another suitable material that could withstand high speed dust grain impacts. This could also be an ablative or a ceramic composite similar to bullet proof vests. For example in the case of the wafersat with a wafer thickness of approximately 100 microns, the outer forward edge could easily be 1cm “wide” by 100 microns thick or perhaps somewhat thicker than the wafer if needed, and still add only a modest amount to the wafer mass. A simpler design that is simpler but twice the shielding mass, though still a small portion of the wafer, is to make the entire outer rim out of shielding. The optimal choice of shield material will need to be designed and tested but this appears to be a promising option.

Spacecraft Perturbation from Dust Impacts – Dust impacts will have a perturbing effect on the spacecraft that becomes increasingly important for lower mass probes. The worst case will be the wafersat case. We can make some estimates of the overall perturbation by comparing the dust impact applied torque impulse and subsequent angular momentum. We will assume a coordinate system where x and y are in the plane of the wafer and z is the normal. The velocity vector is assumed to be along the xz axis of the wafer with the primary component being along the x axis.

For a thin circular disk of uniform mass with total mass m the moment of inertia along the x or y axis is $I_{x,y} = \frac{1}{4} mR^2 = \frac{1}{16} mD^2$ where $R=D/2$ is the disk radius while along the z axis it is $I_z = \frac{1}{2} mR^2 = \frac{1}{8} mD^2$. For a square wafer the moment of inertia is $I_{x,y} = \frac{1}{4} mD^2$ and $I_z = \frac{1}{6} mD^2$ where D is the size of the square side. For a D=10 cm wafer $I_{x,y} = \frac{1}{4} 10^{-3} \text{ (kg)} (0.1\text{m})^2 = 2.5 \times 10^{-6} \text{ kg-m}^2$ (round or square) and $I_z = \frac{1}{8} mD^2$ for round (or $\frac{1}{6} mD^2$ for square) $\sim 1.5 \times 10^{-6} \text{ kg-m}^2$.

The total momentum transfer P_T of an interstellar dust grain impact to the spacecraft, assuming the worst case of an elastic collision again gives $P_{\text{grain}} = 2 m_{\text{grain}} v$ ($=c/3$ here)

For a dust mass of $m_{\text{grain}} \sim 10^{-17} \text{ kg}$ then $P_{\text{grain}} = 2 * 10^{-17} * 10^8 = 2 \times 10^{-9} \text{ N-s}$.

We consider two cases:

- 1) Impact head on but allowed to the dust to hit anywhere along the wafer thickness and allow for a wafer plane misalignment with the velocity vector. If the wafer is 0.1mm thick the applied torsion impulse will be at worst if the impact is at the upper or lower edge impact (0.05mm off centerline). The torque applied is $\tau = \mathbf{r} \times \mathbf{p}$. With a 10 cm wafer (round or square) we get a impulsive torque of $\tau * dt = \frac{1}{2} 10^{-4} \text{ (m)} * 2 \times 10^{-9} \text{ N-s} = 10^{-13} \text{ Nm-s} = I \Delta \omega \rightarrow \Delta \omega = \tau * dt / I \sim 10^{-13} \text{ Nm-s} / 2 \times 10^{-6} \text{ kg-m}^2 = 5 \times 10^{-8} \text{ rad/sec}$. This is extremely small and can be counteracted by the wafer photon thrusters.
- 2) We will assume an initial misalignment of the wafer plane to the velocity vector of 0.001 radians (1 mrad) ~ 200 arc sec. We can do much better than this if needed. As a quick check we see an angular misalignment of 0.001 radians over a 10 cm lever arm gives a displacement at the edge of $0.001 \text{ rad} * 0.1 \text{ m} = 10^{-4} \text{ m}$. This is the thickness of the wafer or 2 times the offset hit in case 1) and thus still leads to a very small impulsive torque and very small $\Delta \omega \sim 2.5 \times 10^{-8} \text{ rad/sec}$ and hence can be corrected by the wafer photon thrusters.

- 3) In this case we allow the dust grain to hit the radial edge so as to cause the wafer to “spin up”. The impulsive torque is $\tau \cdot dt = 0.05\text{m (radius of wafer)} \cdot 2 \times 10^{-9} \text{N-s} = 10^{-10} \text{Nm-s} = I \alpha dt = I d\omega \rightarrow d\omega = \tau \cdot dt / I \sim 10^{-10} \text{Nm-s} / 2 \times 10^{-6} \text{kg-m}^2 = 5 \times 10^{-5} \text{rad/sec}$. This will cause the disk to slowly rotate about the z axis (perpendicular to the wafer xy plane). In one day the wafer will rotate $\sim 5 \times 10^{-5} \text{rad/sec} \cdot 8.6 \times 10^4 \text{s/day}$ about 4.4 rad or close to one revolution. Again this can be counteracted by the wafer photon thrusters.

Onboard and Beamed Power Options – Providing adequate power during the long cruise phase is critical to maintain bidirectional laser communications. This is especially critical with the smaller mass payloads that have extremely limited mass and size for the communications system. We focus on the most difficult case, namely the wafer scale spacecraft. In order to have a reasonable laser communications link from spacecraft to Earth and assuming the main phased array used to drive the spacecraft is also used as a phased array receiver or at least as a light bucket (non phased array receive mode with “light bucket” combining of subelements). We baseline a 1 watt (optical) burst mode transmission (0.5% duty cycle) from the wafersat as the laser comm transmitter. This then requires an average electrical power, assuming 50% conversion efficiency, of about 10 mw. The current baseline is to use a small radio thermal generator (RTG) as the long term on-board power. There are several suitable RTG materials. Pu-238 is one of them. Pu-238 has a half-life of about 87.7 years and produces about $400 \text{mW}_{\text{thermal}}/\text{g}$ initially. Using a Pu-238 RTG and nanowire TE converters allows for an RTG system that has a mass of about 0.3g. The Pu-238 mass can be reduced if the burst power and or duty cycle are reduced. Energy is stored on the wafer using thin film supercapacitors. Such a small system, while theoretically possible, has not been built. Small RTG’s were built for early pacemakers so there is some precedent. The cold background aids the efficiency with an assumed conversion efficiency of 7% or about $30 \text{mW}_{\text{electrical}}/\text{g}(\text{Pu-238})$.

Note that the wafer alone receives significant power from the drive laser if illuminated. A narrow bandgap photo converter (PV) is feasible with greater than 50% efficiency today and this allows the possibility of direct beamed power to the spacecraft for considerable distances. A more advanced option is to coat the drive reflector ($\sim 1 \text{m}^2$) with a narrow bandgap PV would give nearly 100 times the power of the wafer alone. This could conceivably allow beamed power all the way out to the nearest star if the burst fractional time was reduced (see figure below). As the spacecraft approaches a star the onboard PV could be used as a secondary power source. If the approach was close enough this could dominate allowing a much greater burst fraction and hence data rate. Ideally both RTG and PV would be available.

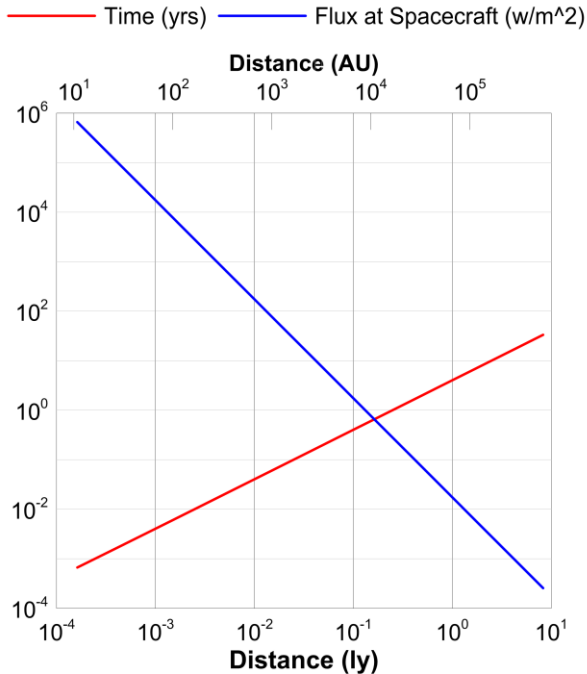


Figure 27 – Flux (w/m²) at spacecraft from DE-STAR and time since launch vs distance(ly). Assume DE-STAR 4 driver with 70 GW.

Photon thrusters – All of the payload designs require some active pointing capability for pointing during laser communications as well as for pointing during imaging and to assume spacecraft orientation to minimize dust impacts to and correct orientation after a dust impact. Small trajectory corrections are also desirable. The baseline is to use photon thrusters to provide the active pointing and guidance capability. Photons give a thrust of P/c or about 3.3 nN/w . Photon thrusters can be accomplished in two ways. One of the use the on-board electrical power to drive small edge mounted laser diodes or LED's. A second way is thermal photons. Assuming the RTG baseline for on-board power there is also the possibility of using the RTG heat, which is ultimately radiated as photons. The effect of the RTG thermal photon thrusting is inevitable even if undesired. Assuming a 7% conversion of thermal to electrical for the RTG, it is clear the thermal effect dominates. A possible way to minimize the RTG thermal effect is to symmetrize the thermal emission of the RTG but it would be useful to take advantage of the much larger RTG thermal photon thruster than to minimize it. Utilizing the RTG thermal photons for thruster control is complicated by the need to control the direction of emission. This could be done with a suitable optical design but it is not a trivial problem. From the RTG calculations we get about $400 \text{ mW}_{\text{thermal}}/\text{g}(\text{Pu-238})$ or about $30 \text{ mW}_{\text{electrical}}/\text{g}$ and ignoring the thermal photons we would get about $10^{-10} \text{ N/g} = 0.1 \text{ nN/g}(\text{Pu-238})$. Note that the electrical power is not only converted into light but also into heat in the laser/LED and this call all be effectively used if designed properly. Hence we can assume near unity conversion efficiency for electrical power to photon thrust. From the calculations of the dust impacts for the edge impacts requiring reorientation we need about 10^{-13} Nm-s of torque impulse per dust grain hit. For the edge hit wafer spin up mode we need about 10^{-10} Nm-s of torque impulse per dust grain hit. Both of these required torque impulses are easily obtained with the photon thrusters even in the wafersat assuming about $0.1 - 0.3 \text{ g}(\text{Pu-238})$ for the hit rates above. For example the edge on hit rate for 10 cm wafer is $R = 10^{-3} \text{ Hz}$ or 1000 sec between hits on average.

Magnetic Torquer - Other possible non expendable orientation control include magnetic torquer that act against the interstellar magnetic field. The interstellar magnetic field is highly anisotropic and

inhomogeneous. A rough estimate is about 1 micro-gauss (0.1 nT) based on the average galactic magnetic field. As an example of such a magnetic torquer would be a single 10cm loop with 1 amp. Using a 0.1nT estimate for the interstellar magnetic field gives a torque of about 10^{-12} N-m (iAB). It is possible to use a thin film current loop with a large number of turns to amplify this effect. 100 turns would not be unreasonable. Using pulsed current from the RTG power source could allow such a system. Since the spacecraft will run very cold during the cruise phase high T_c superconducting films might be an option. Getting 3D control would require a 3 axis torquer. In the case of the wafersat this would be a challenge.

Trajectory modification – The ability to make some modest trajectory modifications would be extremely useful. We assume the use of photon thrusters. We can get an estimate for this but assuming only the use of the electrical portion and not the thermal photon component. The thrust/RTG active mass is 10^{-10} N/g = 0.1nN/ g(Pu-238). Over the course of 1 year this would yield a delta P (momentum) of about 3×10^7 s/yr $\times 10^{-10}$ N/g = 3×10^{-3} N-s/g-yr. Assuming a 1 gram wafer this would give an angular change of $\phi = \text{delta P/P}$ where P is the total momentum with $P = mv \sim 10^{-3}$ (kg) $\times 10^8$ m/s = 10^5 N-s. Thus $\phi = 3 \times 10^{-8}$ rad/g-yr. Assuming a 20 year mission with would yield $\phi_{\text{total}} = 6 \times 10^{-7}$ rad/g. This yields a total displacement D at a distance L of Alpha-Centauri (4.4 ly $\sim 4.4 \times 10^{16}$ m) of $D = L * \phi_{\text{total}} \sim 3 \times 10^{10}$ m/g or about 0.2 AU/g. Using the thermal photons this would increase about 16 times to 3 AU/g. If we assume 0.3 g of Pu0238 we get about 1 AU of displacement over a 20 year mission if we use the thermal photons. This is small but possibly useful.

Payload sizes – Once a suitable laser driver is built the payloads can be any size from miniature relativistic probes, such as the wafer scale one for interstellar flight we have discussed, to large spacecraft capable of transporting humans in the solar system. Some examples of the many mission scenarios possible are shown below. Note the a single laser driver can be used launch sequentially or in parallel any number of spacecraft and thus the system enables and is amortized over a large mission space. The following gives a selected set of possible missions. It is assumed that the reflector mass is equal to the base spacecraft mass (ie system mass not including reflector – or total system mass is twice the base spacecraft mass). The reflector is assumed to be 1 micron thick and the reflector density is assumed to be 1.4 g/cc. The laser array is assumed to be 10km on a side and the reflector is assumed to be square. The mass given is the base spacecraft mass and hence the reflector mass. The laser power is assumed to be 70 GW.

1g – wafer scale spacecraft with 0.85m reflector capable of significant relativistic light.

Time to when laser diffraction spot equals reflector size= 186s

Distance when laser diffraction spot equals reflector size= 4.01×10^9 m

Speed when laser diffraction spot equals reflector size= 4.31×10^7 m/s

Beta when laser diffraction spot equals reflector size=0.14

Speed with continued illumination= 6.10×10^7 m/s

Beta with continued illumination=0.20

Acceleration when reflector is fully illuminated= 2.37×10^{43} g”

10g – multiple wafer scale systems with 2.7m reflector

Time to when laser diffraction spot equals reflector size= 1050s

Distance when laser diffraction spot equals reflector size= 1.27×10^{10} m

Speed when laser diffraction spot equals reflector size= 2.43×10^7 m/s

Beta when laser diffraction spot equals reflector size=0.081
Speed with continued illumination= 3.43×10^7 m/s
Beta with continued illumination=0.11
Acceleration when reflector is fully illuminated= 2.37×10^3 "g"

100g – multiple wafer and sub class CubeSat systems with 8.5m reflector.
Time to when laser diffraction spot equals reflector size= 5880s
Distance when laser diffraction spot equals reflector size= 4.01×10^{10} m
Speed when laser diffraction spot equals reflector size= 1.36×10^7 m/s
Beta when laser diffraction spot equals reflector size=0.046
Speed with continued illumination= 1.93×10^7 m/s
Beta with continued illumination=0.064
Acceleration when reflector is fully illuminated= 237 "g"

1kg – CubeSat class systems with 27m reflector.
Time to when laser diffraction spot equals reflector size= 3.32×10^4 s
Distance when laser diffraction spot equals reflector size= 1.27×10^{11} m
Speed when laser diffraction spot equals reflector size= 7.67×10^6 m/s
Beta when laser diffraction spot equals reflector size=0.026
Speed with continued illumination= 1.08×10^7 m/s
Beta with continued illumination=0.036
Acceleration when reflector is fully illuminated= 23.7 "g"

10kg – significant imaging capability with 85m reflector.
Time to when laser diffraction spot equals reflector size= 1.86×10^5 s
Distance when laser diffraction spot equals reflector size= 4.01×10^{11} m
Speed when laser diffraction spot equals reflector size= 4.31×10^6 m/s
Beta when laser diffraction spot equals reflector size=0.014
Speed with continued illumination= 6.10×10^6 m/s
Beta with continued illumination=0.020
Acceleration when reflector is fully illuminated= 2.37 "g"

100kg – significant robotic mission with multi mission capability with 270m reflector.
Time to when laser diffraction spot equals reflector size= 1.06×10^5 s
Distance when laser diffraction spot equals reflector size= 1.27×10^{12} m
Speed when laser diffraction spot equals reflector size= 2.43×10^6 m/s
Beta when laser diffraction spot equals reflector size=0.0081
Speed with continued illumination= 3.46×10^6 m/s
Beta with continued illumination=0.011
Acceleration when reflector is fully illuminated= 0.237 "g"

1000kg – smallest sized human "shuttle craft" system with 850m reflector.
Time to when laser diffraction spot equals reflector size= 5.88×10^6 s
Distance when laser diffraction spot equals reflector size= 4.01×10^{12} m

Speed when laser diffraction spot equals reflector size= 1.36×10^6 m/s
Beta when laser diffraction spot equals reflector size=0.0046
Speed with continued illumination= 1.93×10^6 m/s
Beta with continued illumination=0.0064
Acceleration when reflector is fully illuminated= 0.0237 "g"

10,000kg – medium human capable or cargo craft for interplanetary travel with 2.7km reflector.
Time to when laser diffraction spot equals reflector size= 3.32×10^7 s
Distance when laser diffraction spot equals reflector size= 1.27×10^{13} m
Speed when laser diffraction spot equals reflector size= 7.67×10^5 m/s
Beta when laser diffraction spot equals reflector size=0.0026
Speed with continued illumination= 1.08×10^6 m/s
Beta with continued illumination=0.0036
Acceleration when reflector is fully illuminated= 2.37×10^{-3} "g"

100,000kg – large human capable or cargo craft for interplanetary travel with 8.5km reflector.
Time to when laser diffraction spot equals reflector size= 1.86×10^8 s
Distance when laser diffraction spot equals reflector size= 4.01×10^{13} m
Speed when laser diffraction spot equals reflector size= 4.31×10^5 m/s
Beta when laser diffraction spot equals reflector size=0.0014
Speed with continued illumination= 6.10×10^5 m/s
Beta with continued illumination=0.0020
Acceleration when reflector is fully illuminated= 2.37×10^{-4} "g"

Roadmap – Should we begin on this path and if so how should we begin. Like any long journey it is easy get discouraged and not take the first steps. There are thousands of reasons not to begin. It is too hard, we are not technologically ready, we will not live to see the final journey to the stars ... Most of these could be said about any profound endeavor. One difference on this journey is we have a very large scale of masses that are relevant to propel to extremely high speed rather than trying to propel a human and while one of the long term goals is to send a probe to a nearby star and return data, this is not the only objective. Part of the starting efforts will be to scope a more complete roadmap from desktop to orbital with an emphasis on understanding the TRL level of each element for future missions. Given the large range between our current chemical propellant propulsion and our goals of relativistic speeds and the range of useful masses from sub gram to large systems, we have an enormous parameter space to work in. All of these are along the path, particularly since this system is modular, scalable and on a very rapid development path and thus lends itself to a roadmap. With laser efficiencies near 50% the rise in efficiency will not be one of the enabling elements along the road map but free space phase control over large distances during the acceleration phase will be. This will require understanding the optics, phase noise and systematic effects of our combined on-board metrology and off-board phase servo feedback. Reflector stability during acceleration will also be on the critical path as will increasing the TRL of the amplifiers for space use. For convenience we break the roadmap into several steps. One of the critical development items for space deployment is greatly lowering the mass of the radiators. While this sounds like a decidedly low tech item to work on, it turns out to be one of the critical mass drivers for space deployment. Current radiators have a mass to radiated power of 25 kg/kw, for radiated temperatures near 300K. This is an area where some new ideas are needed. With our current Yb fiber baseline laser

amplifier mass to power of 5kg/kw (with a likely 5 year roadmap to 1 kg/kw) and current space photovoltaics of less than 7 kg/kw, the radiators are a serious issue for large scale space deployment.

Technology Maturation:

Laser and Phased Array

- Increase TRL of laser amplifiers to at least TRL 6
- Test of low mass thin film optics as an option
- Reduce SBS effect to lower bandwidth and increase coherence time/ length
- Optimize multiple lower power amplifiers vs fewer higher power units – SBS/coherence trades
- Maturation and miniaturization of phase control elements for phased array
- Phase tapping and feedback on structure
- Structural metrology designs
- Study of optimized Kalman filters as part of phase control and servo targeting loop
- Study and test near field phase feedback from small free-flyer elements
- Study beam profiling and methods to smooth beam on reflector
- Beam randomization techniques to flatten beam

Reflector

- Study multilayer dielectric coating to minimize loss and maximize reflectivity – trade study
- Study materials designs for minimal mass reflectors – plastics vs glasses
- Shape designs for reflector stability - shaping
- Study designs with varying thicknesses and dielectric layers
- Study designs with low laser line absorption and high thermal IR absorption (emission)
- Study broader band reflectors to deal with relativistic wavelength shift with speed
- Study self stabilizing designs
- Simulations of reflector stability and oscillations during acceleration phase – shape changes
- Study spinning reflector to aid stability and randomization of differential force and heating
- Study techniques for reflector to laser active feedback
- Study techniques to keep beam on reflector

Wafer scale spacecraft

- Study materials for lowest power and high radiation resistance and compatibility with sensors
- Determine power requirements
- Study onboard power options – RTG, beta converter, beamed power
- Design narrow bandgap PV for beamed power phase
- Design on-wafer laser communications
- Design optical and IR imaging sensors
- Star tracker and laser lock modes
- Study swarm modes including intercommunications
- Design watchdog timers and redundant computational and sensor/ power topologies

- Test in beam line to simulate radiation exposure
- Design on-board or thin film “pop up” optics
- Design fiber optic or similar cloaking to mitigate heating during laser exposure
- Simulate thermal management both during laser exposure and during cruise phase
- Simulate radiation exposure during cruise phase
- Study materials for lowest power and high radiation resistance and compatibility with sensors
- Simulate imaging of target objects
- Study use of WaferSat for planetary and terrestrial probes

Communications

- Optimize wafer only laser communications
- Study feasibility of using acceleration reflector as part of laser communications
- Study feasibility of using reflector as thin film optics for laser comm and imaging

System Level

- Detailed design studies including mass tradeoffs and costing vs system size
- Develop cost roadmaps identifying critical elements as impediments to deployment vs size
- Design, build, test ground based structures with metrology feedback system
- Design and simulate orbital structures of various sizes (fixed vs sub element free flyer)
- Study orbital tradeoffs and project launcher feasibility vs time
- Study LEO, GEO, Lagrange points, lunar options
- Simulations of prober orbital trajectories including any Earth blockage effects
- Work with space PV designers to optimize efficiency and minimize mass
- Develop PV roadmap for mass, efficiency, rad resistance and aging
- Develop roadmap to reducing radiator mass by 10x as goal.
- Study target selection of possible exoplanet systems
- Study solar system targets
- Study multi mode use including space debris, beamed power, SPS, planetary defense ...
- International space law issues

Operational Maturation and Steps:

- Step 1 - Ground based - Small phased array, beam targeting and stability tests - 10 kw
- Step II – Ground based - Target levitation and lab scale beam line acceleration tests - 10 kw
- Step III – Ground based - Beam formation at large array spacing –
- Step IV – Ground based - Scale to 100 kW with arrays sizes in the 1-3 m size –
- Step V – Ground based - Scale to 1 MW with 10 m optics –
- Step VI – Orbital testing with small 1-3 class arrays and 10-100kw power – ISS possibility
- Step VII – Orbital array assembly tests in 10 m class array
- Step VIII – Orbital assembly with sparse array at 100 m level –
- Step IX – Orbital filled 100 m array
- Step X – Orbital sparse 1km array
- Step XI – Orbital filled 1 km array

Step XII – Orbital sparse 10 km array
Step XIII – Orbital filled 10 km array

Other Benefits. As we outline in our papers the same basic system can be used for many purposes including both stand-on and stand-off planetary defense from virtually all threats with rapid response, orbital debris mitigation, orbital boosting from LEO to GEO for example, future ground to LEO laser assisted launchers, standoff composition analysis of distant object through molecular line absorption, active illumination of asteroids and other solar system bodies, beamed power to distant spacecraft among others. The same system can also be used for beaming power down to the Earth via micro or mm waves for selected applications. This technology will give us transformative options that are not possible now and allows us to go far beyond our existing chemical propulsion systems.

ACKNOWLEDGEMENTS

We gratefully acknowledge funding from the NASA California Space Grant NASA NNX10AT93H in support of this research.

Appendix

Laser Sail - Non Relativistic solution

Assume square sail with thickness h , size D , density ρ , bare (no sail) payload mass m_0

Distance to sail = d

Assume perfect reflectivity - $\epsilon_R = 1$

Distance from laser to sail = L

Spot size is D_s

$$\theta = 2\lambda / d$$

$$D_s = \text{spot size} = L\theta = \frac{2L\lambda}{d}$$

$F = \text{force - thrust on sail}$

$$F = 2P_0 / c \text{ for } D_s < D$$

$$F = \frac{2P_0}{c} \left(\frac{D}{D_s} \right)^2 = \frac{P_0}{2c} \frac{d^2 D^2}{L^2 \lambda^2}$$

1) $D_s < D$ $L_0 =$ distance where spot size = sail size

$$L_0 \theta = D = \frac{2\lambda L_0}{d} \rightarrow L_0 = \frac{dD}{2\lambda}$$

$F = \frac{2P_0}{c}$ is constant while $D_s < D$

$$FL_0 = (\text{energy to distance } L_0) = KE = \frac{1}{2}mv^2$$

$$v = \sqrt{\frac{2FL_0}{m}} = \sqrt{2aL_0}$$

$$a = F / m$$

$$m = m_{sail} + m_0$$

$$m_{sail} = D^2 h \rho$$

$$KE = FL_0 = \frac{2P_0}{c} \frac{dD}{2\lambda} = \frac{P_0 d D}{c \lambda}$$

$$v(L) = \sqrt{\frac{4P_0 L}{c(D^2 h \rho + m_0)}}$$

$$v = v_0 \text{ when } L = L_0$$

$$v_0 = \left(\frac{4P_0 L_0}{c(D^2 h \rho + m_0)} \right)^{1/2} = \left(\frac{2P_0 d D}{c \lambda (D^2 h \rho + m_0)} \right)^{1/2}$$

$$a = F / m = \frac{2P_0}{(D^2 h \rho + m_0)c} = \text{is constant while } D_s < D$$

$$t(L) = v(L) / a = \left(\frac{Lc(D^2 h \rho + m_0)}{P_0} \right)^{1/2}$$

$$t_0 = v_0 / a = \left(\frac{L_0 c (D^2 h \rho + m_0)}{P_0} \right)^{1/2} = \left(\frac{cdD(D^2 h \rho + m_0)}{2P_0 \lambda} \right)^{1/2}$$

$$t_0 = \text{time to } v = v_0$$

If $m_0 = 0$ (no payload mass) then

$$m = m_{sail} = D^2 h \rho$$

$$v(L) = \sqrt{\frac{4P_0 L}{cD^2 h \rho}}$$

$$v = v_0 \text{ when } L = L_0$$

$$v_0 \propto h^{-1/2}, P_0^{1/2}, d^{1/2}, D^{-1/2}, \lambda^{-1/2}, \rho^{-1/2}$$

$$v_0 = \left(\frac{4P_0 L_0}{cD^2 h \rho} \right)^{1/2} = \left(\frac{2P_0 d D}{c \lambda D^2 h \rho} \right)^{1/2}$$

$$a = \frac{2P_0}{D^2 h \rho c} \quad v \propto P_0, D^{-2}, h^{-1}, \rho^{-1}$$

$$t(L) = v(L) / a = \left(\frac{L c D^2 h \rho}{P_0} \right)^{1/2}$$

$$t_0 = v_0 / a = \left(\frac{L_0 c D^2 h \rho}{P_0} \right)^{1/2} = \left(\frac{c d D D^2 h \rho}{2 P_0 \lambda} \right)^{1/2} = \left(\frac{c d D^3 h \rho}{2 P_0 \lambda} \right)^{1/2} \quad t_0 \propto P_0^{-1/2}, d^{1/2}, D^{3/2}, h^{1/2}, \lambda^{-1/2}, \rho^{1/2}$$

Note that $v_0 \propto d^{1/2}, D^{-1/2}, h^{-1/2}$ implies that a smaller reflector is faster

$$\text{Why is a smaller reflector faster? } v_0 = \left(\frac{2KE}{m} \right)^{1/2} = \left(\frac{2FL_0}{m} \right)^{1/2}$$

$$m \propto D^2, L_0 \propto D \text{ F is constant so } v_0 \propto \frac{1}{\sqrt{D}}$$

I we want high v => make D small.

Smaller sail is faster IF $m_0 = 0$. Make sail as small as possible IF highest speed is the metric and if $m_0 = 0$.

With continued illumination, beyond when the laser spot exceeds the reflector size, the speed increases by $\sqrt{2}$ larger than $v_0 \rightarrow v_\infty \equiv v(L = \infty) = \sqrt{2}v_0$

$$2) D_s > D, \quad F = \frac{2P_0}{c} \left(\frac{D}{D_s} \right)^2 = \frac{P_0}{2c} \frac{d^2 D^2}{L^2 \lambda^2} = \frac{2P_0}{c} \left(\frac{L_0}{L} \right)^2$$

a) $D_s < D$

$$\left(L_0 = \frac{d D_s}{2 \lambda} \right)$$

$$KE_1 (\text{from } L = 0 \text{ to } L_0, D_s = D \text{ or } L = L_0) = FL_0$$

$$= 2 \frac{P_0}{c} L_0 = \frac{P_0 d D}{c \lambda}$$

L_0 is the distance at which $D = D_s$

b) KE_2 from $L = L_0$ to ∞

$$\begin{aligned}
KE_2 &= \int_{L_0}^{\infty} F dL = \frac{P_0 d^2 D^2}{2c\lambda^2} \int_{L_0}^L \frac{dL}{L^2} = \frac{P_0 d^2 D^2}{2c\lambda^2} \left(\frac{1}{L_0} - \frac{1}{L} \right) \\
&= KE_1 \frac{dD}{2\lambda} \left(\frac{1}{L_0} - \frac{1}{L} \right) = KE_1 L_0 \left(\frac{1}{L_0} - \frac{1}{L} \right) = KE_1 \left(1 - \frac{L_0}{L} \right) \rightarrow KE_1 \text{ ie } KE_2 = KE_1 \text{ as } L \text{ goes to } \infty
\end{aligned}$$

$$KE_{total} = KE_1 + KE_2 = KE_1 (2 - L_0 / L) = \frac{2P_0}{c} L_0 (2 - L_0 / L)$$

$$\rightarrow 2KE_1 = \frac{2P_0 dD}{c\lambda} = \frac{4P_0}{c} \frac{dD}{2\lambda}$$

$$= \frac{4P_0}{c} L_0 = \frac{2P_0}{c} 2L_0 = F * 2L_0 = \frac{1}{2} mv^2, L \rightarrow \infty$$

$$v(L) = \left[\frac{2P_0 dD}{mc\lambda} (2 - L_0 / L) \right]^{1/2} = \left[\frac{4P_0}{mc} L_0 (2 - L_0 / L) \right]^{1/2}$$

$$v_0 = v(L = L_0) = \left[\frac{2P_0 dD}{mc\lambda} \right]^{1/2} = \left[\frac{4P_0}{mc} L_0 \right]^{1/2} = [2a_0 L_0]^{1/2}$$

$$\text{where } a_0 = F / m = \frac{2P_0}{mc}$$

$$v(L) = \left[\frac{2P_0 dD}{mc\lambda} (2 - L_0 / L) \right]^{1/2} = v_0 [(2 - L_0 / L)]^{1/2}$$

$$v_{\infty} \equiv v(L = \infty) = \sqrt{2} v_0$$

$$L_0 = dD / 2\lambda$$

$$a(L) = F(L) / m = \frac{P_0}{2mc} \left(\frac{dD}{L\lambda} \right)^2 = \frac{2P_0}{mc} \left(\frac{L_0}{L} \right)^2 = a_0 \left(\frac{L_0}{L} \right)^2$$

$$v(L) = \left(\frac{2P_0 dD}{c\lambda(m_{sail} + m_0)} \right)^{1/2} [(2 - L_0 / L)]^{1/2} = \left(\frac{2P_0 dD}{c\lambda(D^2 h \rho + m_0)} \right)^{1/2} [(2 - L_0 / L)]^{1/2} \text{ for } L > L_0$$

Maximizing Speed of Laser driven system

Let $v = v(L)$

For $L = L_0, v(L_0) \equiv v_0 = v_0(D)$

$$L_0 = dD / 2\lambda$$

where D is the sail size and $L = L_0$ when spot size = D

$$\begin{aligned} v_0(D) &= \left(\frac{2P_0 d}{c\lambda} \right)^{1/2} \left(\frac{D}{D^2 h \rho + m_0} \right)^{1/2} \\ &= \left(\frac{2P_0 d}{c\lambda} \right)^{1/2} \left(\frac{D}{m_s + m_0} \right)^{1/2} \end{aligned}$$

where $m_s = \text{mass sail} = D^2 h \rho$

$m_0 = \text{payload mass without sail}$

$v(D)$ limiting cases:

$$v_0(D=0) = 0$$

$$\lim_{D \rightarrow \infty} v_0(D) = 0$$

hence find D to give maximum v_0

$$\text{set } dv / dD = 0$$

$$dv / dD = 1/2 \left(\frac{D}{D^2 h \rho + m_0} \right)^{-1/2} \left(\frac{D^2 h \rho + m_0 - D(2Dh\rho)}{(D^2 h \rho + m_0)^2} \right) = 1/2 \left(\frac{D}{m_s + m_0} \right)^{1/2} \left(\frac{m_0 - m_s}{(m_s + m_0)^2} \right)$$

Therefore max v ($dv/dD=0$) occurs when $m_s = m_0$ (mass sail = payload mass)

Therefore:

$$v_{0max}(m_s = m_0) = \left(\frac{2P_0 d}{c\lambda} \right)^{1/2} \left(\frac{D}{2m_0} \right)^{1/2} = \left(\frac{P_0 d}{c\lambda} \right)^{1/2} (h\rho m_0)^{-1/4}$$

(since $D = (m_0 / h\rho)^{1/2}$ for $m_{sail} = m_0$)

$$= \left(\frac{P_0 d}{c\lambda} \right)^{1/2} (h\rho D)^{-1/2}$$

$$= \left(\frac{P_0}{c\lambda h\rho} \right)^{1/2} \left(\frac{d}{D} \right)^{1/2}$$

$$= c \left(\frac{P_0}{P_1} \right)^{1/2} \left(\frac{d}{D} \right)^{1/2}$$

where $P_1 \equiv c^3 \lambda h \rho \approx 2.7 \times 10^{16}$ watts $\times \lambda(\text{microns}) h(\text{microns}) \rho(\text{g/cc})$

$II(L = \infty)$

$$\lim_{L \rightarrow \infty} v(L) \equiv v_{\infty} = v_0 \sqrt{2}$$

$$dv / dD(L = \infty) = 0 = dv / dD(L = L_0) \sqrt{2}$$

therefore same condition for max v -ie when $m_s = m_0$

$$\rightarrow \lim_{L \rightarrow \infty} v(L) \equiv v_{\infty} = v_0 \sqrt{2} = \left(\frac{2P_0 d}{c \lambda} \right)^{1/2} (h \rho m_0)^{-1/4}$$

$III(a, t @ v_{0max} (m_s = m_0) \rightarrow m = m_s + m_0 = 2m_s = 2m_0)$

$$a = \frac{F}{m} = \frac{F}{2m_0} = \frac{P_0}{m_0 c} = \frac{P_0}{c D^2 h \rho}$$

$$t_0 = \frac{v_{0max}}{a} = \left(\frac{cdD^3 h \rho}{P_0 \lambda} \right)^{1/2} = \left(\frac{cdDD^2 h \rho}{P_0 \lambda} \right)^{1/2} = \left(\frac{cdDm_0}{P_0 \lambda} \right)^{1/2} = \left(\frac{2cL_0 m_0}{P_0} \right)^{1/2} = \left(2 \frac{m_0 c^2 L_0}{P_0 c} \right)^{1/2}$$

$$t_0 = \left(\frac{cdDm_0}{P_0 \lambda} \right)^{1/2} = \left(\frac{cd}{P_0 \lambda} \right)^{1/2} \left(\frac{m_0^3}{h \rho} \right)^{1/4}$$

$$D = (m_0 / h \rho)^{1/2}$$

$$L_0 = dD / 2 \lambda$$

t_0 is time when spot size = sail size

Effect of imperfect reflector

If the reflector has non unity reflection coefficient ϵ_r then P_0 above is replaced by $P_0(1 + \epsilon_r)/2$ where ϵ_r is the reflection coefficient.

Relativistic Solution

A first order relativistic solution is given below. A more complete solution is given in Kulkarni and Lubin (2016)

$$p = \text{momentum} = m_0 \gamma v$$

$$\gamma = (1 - \beta^2)^{-1/2} \quad \text{where} \quad \beta = \frac{v}{c}$$

$$\gamma = \frac{1}{\sqrt{1 - (v/c)^2}} = (1 - \beta^2)^{-1/2} \rightarrow 1 + \frac{1}{2} \beta^2, \beta \ll 1$$

$$F = \frac{dp}{dt} = \frac{2P\varepsilon_r}{c} + \frac{P(1-\varepsilon_r)}{c} = \frac{P(1+\varepsilon_r)}{c} \quad P = \text{Laser power at reflector}$$

$\varepsilon_r =$ Re flector reflection coef

$\varepsilon_r = 1$ for perfect reflection

$\varepsilon_r = 0$ for perfect absorption

$P = \frac{P_0}{\gamma} =$ power at reflector (freq of photons and hence power reduced by γ)

$P_0 =$ Transmitted power

$$F = \frac{P_0(1+\varepsilon_r)}{\gamma c} = dp / dt = m_0 \frac{d}{dt}(\gamma v) = m_0 \left(\frac{d\gamma}{dt} v + \gamma \frac{dv}{dt} \right)$$

$$= m_0 \left(\frac{d\gamma}{dv} \frac{dv}{dt} v + \gamma \frac{dv}{dt} \right) = m_0 \left(\frac{d\gamma}{dv} v + \gamma \right) \frac{dv}{dt}$$

$$\rightarrow \frac{dv}{dt} = \frac{P_0(1+\varepsilon_r)}{m_0 c} \frac{1}{\gamma \left(\frac{d\gamma}{dv} v + \gamma \right)}$$

$$\gamma = (1-\beta^2)^{-1/2}$$

$$\frac{d\gamma}{dv} = \frac{-1}{2} (1-\beta^2)^{-3/2} (-2\beta \frac{d\beta}{dv}) = \gamma^3 \frac{\beta}{c} = \gamma^3 \frac{v}{c^2}$$

$$\gamma \left(\frac{d\gamma}{dv} v + \gamma \right) = \gamma (\gamma^3 \beta^2 + \gamma) = \gamma^2 (\gamma^2 \beta^2 + 1) = \gamma^4$$

$$\gamma^2 \beta^2 + 1 = \left(\frac{\beta^2}{1-\beta^2} \right) + 1 = \frac{\beta^2 + (1-\beta^2)}{1-\beta^2} = \frac{1}{1-\beta^2} = \gamma^2$$

$$\rightarrow \frac{dv}{dt} = \frac{P_0(1+\varepsilon_r)}{m_0 c \gamma^4}$$

$$\rightarrow \gamma^4 dv = \frac{P_0(1+\varepsilon_r)}{m_0 c} dt$$

$$\rightarrow \frac{dv}{\left(1-(v/c)^2\right)^2} = \frac{P_0(1+\varepsilon_r)}{m_0 c} dt$$

$$t = \int dt = \frac{m_0 c}{P_0(1+\varepsilon_r)} \int \frac{dv}{\left[\left(1-(v/c)^2\right)\right]^2} = \frac{m_0 c^2}{P_0(1+\varepsilon_r)} \int \frac{d\beta}{(1-\beta^2)^2}$$

$$\text{Note: } \int \frac{dv}{\left[\left(1-(v/c)^2\right)\right]^2} = \int \gamma^4 dv$$

$$= \frac{m_0 c^2}{2P_0(1+\varepsilon_r)} \left[\frac{\beta}{1-\beta^2} + \frac{1}{2} \ln \left| \frac{1+\beta}{1-\beta} \right| \right] = \frac{m_0 c^2}{2P_0(1+\varepsilon_r)} \left[\gamma^2 \beta + \tanh^{-1} \beta \right]$$

$$\ln \left(\frac{1+\beta}{1-\beta} \right) = \sum_1^{\infty} \frac{2}{2n-1} \beta^{2n-1} \rightarrow 2\beta \quad (\beta \ll 1)$$

$$\rightarrow t \rightarrow \frac{m_0 c^2}{2P_0(1+\varepsilon_r)} [\beta + \beta] = m_0 v \frac{c}{P_0(1+\varepsilon_r)} = \frac{m_0 v}{F} = \frac{p}{F} \quad \beta \ll 1 \rightarrow \text{consistent}$$

$$v = (F / m_0) t = at$$

$$\text{Note } \ln \left(\frac{1+\beta}{1-\beta} \right) = 2 \tanh^{-1} \beta \quad \tanh^{-1}(x) \sim x \quad x \ll 1$$

$$\text{Define } t_E \equiv \frac{m_0 c^2}{P_0} \rightarrow t = \frac{t_E}{2(1+\varepsilon_r)} \left[\gamma^2 \beta + \tanh^{-1} \beta \right]$$

References

- Bae, Y. K. (2012), "Prospective of photon propulsion for interstellar flight," *Physics Procedia* 38, 253-279.
- Beals, K. A., Beaulieu, M., Dembia, F. J., Kerstiens, J., Kramer, D. L., West, J. R., and Zito, J. A. (1988), "Project Longshot: An Unmanned Probe to Alpha Centauri," US Naval Academy, NASA-CR-184718.
- Bible, J., Bublitz, J., Johansson, I., Hughes, G.B., and Lubin, P. "Relativistic Propulsion Using Directed Energy," *Nanophotonics and Macrophotonics for Space Environments VII*, edited by Edward W. Taylor, David A. Cardimona, Proc. of SPIE Vol. 8876, 887605 (2013).
- Bond, A., and Martin, A. R. (1978), "Project Daedalus - Final Report," *Journal of the British Interplanetary Society Supplement*, 5-7.
- Bussard, R. (1958), "Concepts for Future Nuclear Rocket Propulsion," *Journal of Jet Propulsion* 28, 223-227.
- Curtin, B., Bowers, J., "Thermoelectric power factor enhancement with gate-all-around silicon nanowires," *Journal of Applied Physics* 115, 143704 (2014); doi: 10.1063/1.4870962
- Forward, R. L. (1984), "Roundtrip interstellar travel using laser-pushed lightsails," *Journal of Spacecraft and Rockets* 21, 187-195.
- Forward, R. L. (1985), "Antiproton annihilation propulsion," *Journal of Propulsion and Power* 1, 370-374.
- Hughes, G.B., Lubin, P., O'Neill, H., Meinhold, P., Suen, J., Riley, J., Johansson Hummelgård, I., Bible, J., Bublitz, J., Arriola, J., Motta, C., Griswold, J., Cook, B., Sarvian, N., Clayton-Warwick, D., Wu, J., Milich, A., Oleson, M., Kangas, M., Pryor, M. and Krogen, P. "DE-STAR: phased-array laser technology for planetary defense and exploration," *STARDUST 1st Stardust Global Virtual Workshop on Asteroids and Space Debris 2014*, *Advances in Space Research - Special Edition: Asteroids and Space Debris*, published by Elsevier edited by Massimiliano Vasile (in press 2015).
- Hughes, G.B., Lubin, P., Griswold, J., Bozinni, D., O'Neill, H., Meinhold, P., Suen, J., Bible, J., Riley, J., Johansson, I., Pryor, M. and Kangas, M. "Optical modeling for a laser phased-array directed energy system (Invited Paper)," *Nanophotonics and Macrophotonics for Space Environments VIII*, edited by Edward W. Taylor, David A. Cardimona, Proc. of SPIE Vol. 9226 (Aug, 2014).
- Hughes, G.B., Lubin, P., Bible, J., Bublitz, J., Arriola, J., Motta, C., Suen, J., Johansson, I., Riley, J., Sarvian, N., Wu, J., Milich, A., Oleson, M., and Pryor, M. "DE-STAR: phased-array laser technology for planetary defense and other scientific purposes (Keynote Paper)," *Nanophotonics and Macrophotonics for Space Environments VII*, edited by Edward W. Taylor, David A. Cardimona, Proc. of SPIE Vol. 8876, 88760J (Aug, 2013).
- J. C. Hulme, J. K. Doyle, M. J. R. Heck, J. D. Peters, M. L. Davenport, J. T. Bovington, L. A. Coldren, and J. E. Bowers, "Fully integrated hybrid silicon free-space beam steering source with 32 channel phased array," An Invited Paper at the 2014 SPIE Conference
- Johansson, I., Tsareva, T., Griswold, J., Lubin, P., Hughes, G.B., O'Neill, H., Meinhold, P., Suen, J., Zhang, Q., J., Riley, J. Walsh, K., Mellis, C., Brashears, T., Bollag, J., Matthew, S. and Bible, J. "Effects of asteroid rotation on directed energy deflection," *Nanophotonics and Macrophotonics for*

- Space Environments VIII*, edited by Edward W. Taylor, David A. Cardimona, Proc. of SPIE Vol. 9226 (Aug, 2014).
- Kosmo, K., Lubin, P., Hughes, G.B., J., Griswold, Zhang, Brashears, T. “Directed Energy Planetary Defense,” *to be published in IEEE Aerospace 2015 - Asteroid Hazard Detection, Mitigation and Retrieval Concepts (in press 2015)*
- Kosmo, K., Pryor, M., Lubin, P., Hughes, G.B., O’Neill, H., Meinhold, P., Suen, J., C., Riley, J., Griswold, J., Cook, B.V., Johansson, I.E., Zhang, Q., Walsh, K., Melis, C., Kangas, M., Bible, J., Motta, Brashears, T., Mathew, S. and Bollag, J. “DE-STARLITE - a practical planetary defense mission,” *Nanophotonics and Macrophotonics for Space Environments VIII*, edited by Edward W. Taylor, David A. Cardimona, Proc. of SPIE Vol. 9226 (Aug, 2014).
- Lubin, P., Hughes, G.B., Bible, J., Bublitz, J., Arriola, J., Motta, C., Suen, J., Johansson, I., Riley, J., Sarvian, N., Clayton-Warwick, D., Wu, J., Milich, A., Oleson, M., Pryor, M., Krogen, P., Kangas, M., and O’Neill, H. “Toward directed energy planetary defense,” *Optical Engineering*, Vol. 53, No. 2, pp 025103-1 to 025103-18 (Feb 2014), doi: 10.1117/1.OE.53.2.025103.
- Lubin, P., Hughes, G.B.J., Bible, J., Johansson Hummelgård, I., “Directed Energy for Planetary Defense and exploRation - Applications to Relativistic Propulsion and Interstellar Communications” edited by Gerald Cleaver - *Journal of the British Interplanetary Society (JBIS) (in press 2015)*
- Lubin, P., Hughes, G.B. - invited chapter on “Directed Energy for Planetary Defense” - *Handbook of Cosmic Hazards and Planetary Defense - Springer Verlag book (2015)*
- Lubin, P. “The Search for Directed Intelligence” - *Journal of the British Interplanetary Society (JBIS) (submitted 2015, expected publication 2016)*
- Lubin, P., Hughes, G.B., Bible, J., Bublitz, J., Arriola, J., Motta, C., Suen, J., Johansson, I., Riley, J., Sarvian, N., Clayton-Warwick, D., Wu, J., Milich, A., Oleson, M., Pryor, M., Krogan, P. and Kangas, M. “Directed energy planetary defense (Plenary Paper),” *Nanophotonics and Macrophotonics for Space Environments VII*, edited by Edward W. Taylor, David A. Cardimona, Proc. of SPIE Vol. 8876, 887602 (Aug, 2013).
- Kulkarni, N and Lubin, P. “Relativistic Directed Energy Reflector”, in progress
- Riley, J., Lubin, P., Hughes, G.B., O’Neill, H., Meinhold, P., Suen, J., Bible, J., Johansson, I., Griswold, J. and Cook, B. “Directed energy active illumination for near-Earth object detection,” Conditionally Accepted for publication by *Journal of Astronomical Telescopes, Instruments and Systems* (Oct, 2014).
- Riley, J., Lubin, P., Hughes, G.B., O’Neill, H., Meinhold, P., Suen, J., Bible, J., Johansson, I., Griswold, J. and Cook, B. “Directed energy active illumination for near-Earth object detection,” *Nanophotonics and Macrophotonics for Space Environments VIII*, edited by Edward W. Taylor, David A. Cardimona, Proc. of SPIE Vol. 9226 (Aug, 2014).
- Zhang, Q., Walsh, K., Mellis, C., Hughes, G.B., Lubin, P. “Orbital Simulations of Directed Energy Deflection of Near-Earth Asteroids” to be published in *13th Hypervelocity Impact Symposium* (in press 2015).
- Zhang et al "Orbital Simulations of Laser Driven Probes" *Nanophotonics and Macrophotonics for Space Environments*, SPIE Aug 2015